




Corticocortical innervation subtypes of layer 5 intratelencephalic cells in the murine secondary motor cortex

Sanghun Im ^{1,2,3}, Yoshifumi Ueta ⁴, Takeshi Otsuka^{1,2}, Mieko Morishima^{1,5}, Mohammed Youssef^{1,6}, Yasuharu Hirai⁷, Kenta Kobayashi⁸, Ryosuke Kaneko^{9,10}, Kenji Morita^{11,12}, Yasuo Kawaguchi ^{1,2,3,*}

¹National Institute for Physiological Sciences (NIPS), Okazaki 444-8787, Japan,

²Department of Physiological Sciences, The Graduate University for Advanced Studies (SOKENDAI), Okazaki 444-8787, Japan,

³Brain Science Institute, Tamagawa University, Machida, Tokyo 194-8610, Japan,

⁴Department of Physiology, Division of Neurophysiology, School of Medicine, Tokyo Women's Medical University, Tokyo 162-8666, Japan,

⁵Institute of Clinical Medicine and Research, Jikei University School of Medicine, Chiba 277-8567, Japan,

⁶Department of Animal Physiology, Faculty of Veterinary Medicine, South Valley University, Qena 83523, Egypt,

⁷Laboratory of Histology and Cytology, Faculty of Medicine, Hokkaido University, Sapporo 060-8638, Japan,

⁸Section of Viral Vector Development, National Institute for Physiological Sciences, Okazaki 444-8585, Japan,

⁹Bioresource Center, Gunma University Graduate School of Medicine, Gunma 371-8511, Japan,

¹⁰KOKORO-Biology Group, Laboratories for Integrated Biology, Graduate School of Frontier Biosciences, Osaka University, Osaka 565-0871, Japan,

¹¹Physical and Health Education, Graduate School of Education, The University of Tokyo, Tokyo 113-0033, Japan,

¹²International Research Center for Neurointelligence (WPI-IRCN), The University of Tokyo, Tokyo 113-0033, Japan

*Corresponding author: Brain Science Institute, Tamagawa University Machida, Tokyo 1948610, Japan. Email: e191574@eve.tamagawa.ac.jp

Feedback projections from the secondary motor cortex (M2) to the primary motor and sensory cortices are essential for behavior selection and sensory perception. Intratelencephalic (IT) cells in layer 5 (L5) contribute feedback projections to diverse cortical areas. Here we show that L5 IT cells participating in feedback connections to layer 1 (L1) exhibit distinct projection patterns, genetic profiles, and electrophysiological properties relative to other L5 IT cells. An analysis of the MouseLight database found that L5 IT cells preferentially targeting L1 project broadly to more cortical regions, including the perirhinal and auditory cortices, and innervate a larger volume of striatum than the other L5 IT cells. We found experimentally that in upper L5 (L5a), ER81 (ETV1) was found more often in L1-preferring IT cells, and in IT cells projecting to perirhinal/auditory regions than those projecting to primary motor or somatosensory regions. The perirhinal region-projecting L5a IT cells were synaptically connected to each other and displayed lower input resistance than contra-M2 projecting IT cells including L1-preferring and nonpreferring cells. Our findings suggest that M2-L5a IT L1-preferring cells exhibit stronger ER81 expression and broader cortical/striatal projection fields than do cells that do not preferentially target L1.

Key words: intratelencephalic pyramidal cell; corticocortical; corticostriatal; MouseLight; ER81.

Introduction

Higher-order areas of the frontal cortex receive various kinds of information from sensory areas (feedforward pathways) and, in turn, send information about motor plans or outputs back to primary motor (M1) and sensory cortices (feedback pathways; [Barbas and Rempel-Clower 1997](#); [Shipp 2005](#); [Yeterian et al. 2012](#); [Barbas 2015](#)). These feedback signals are important for behavioral selection and sensory perception ([Bastos et al. 2012](#); [Shipp et al. 2013](#); [Mejias et al. 2016](#)). In general, feedback projections are typically thought to involve layer 5 (L5) pyramidal cells (PCs) projecting preferentially to layer 1 (L1) and layer 5/6 of lower-order cortical areas ([Felleman and Van Essen 1991](#); [Markov et al. 2014](#); [D'Souza and Burkhalter 2017](#)). However, L5 PCs are diverse in physiological,

morphological, and molecular markers, suggesting that feedback circuits may also be heterogeneous ([Harris and Shepherd 2015](#); [Ramaswamy and Markram 2015](#); [Kawaguchi 2017](#); [Baker et al. 2018](#); [Tasic et al. 2018](#)). To better understand the role of corticocortical feedback, it will be important to identify the L5 PC subtypes that participate in the projections ([Harris et al. 2019](#)).

In rodents, the secondary motor cortex (M2) projects to primary motor and diverse sensory cortical areas ([Ueta et al. 2014](#); [Manita et al. 2015](#); [Barthas and Kwan 2017](#); [Kawaguchi 2017](#); [Makino et al. 2017](#); [Lin et al. 2018](#)). There are two major PC subtypes in M2-L5: pyramidal tract (PT) cells projecting to the pontine nuclei (corticopontine, or CPn, cells) and intratelencephalic (IT) cells projecting to the contralateral cortex. These subtypes have dis-

Received: March 15, 2021. **Revised:** January 25, 2022. **Accepted:** January 26, 2022

© The Author(s) 2022. Published by Oxford University Press on behalf of The Institute of Mathematics and its Applications. All rights reserved. For permissions, please email: journals.permissions@oup.com

This is an Open Access article distributed under the terms of the Creative Commons Attribution-NonCommercial License (<http://creativecommons.org/licenses/by-nc/4.0/>), which permits non-commercial re-use, distribution, and reproduction in any medium, provided the original work is properly cited. For commercial re-use, please contact journals.permissions@oup.com

tinct morphological and physiological characteristics as well as connection properties (Morishima and Kawaguchi 2006; Otsuka and Kawaguchi 2008; Morishima et al. 2011; Kiritani et al. 2012; Ushimaru and Kawaguchi 2015). Both L5 PC subtypes innervate L1 of M2 as well as the primary motor cortex (Hirai et al. 2012; Ueta et al. 2013). However, L5 IT cells innervate more diverse cortical areas (e.g. perirhinal cortex) than CPn cells (Ueta et al. 2013) and are thought to be more differentiated according to their target cortical areas (Otsuka and Kawaguchi 2011). Furthermore, L5 IT cells within the motor cortex display heterogeneous morphological, physiological, and molecular characteristics (Otsuka and Kawaguchi 2011; Ueta et al. 2013; Tantarigama et al. 2014). Determining whether the diversity of corticocortical feedback projections from M2-L5 IT cells is associated with intrinsic characteristics and connection properties will facilitate our understanding of corticocortical feedback circuits.

To elucidate the corticocortical projection characteristics of M2-L5 IT cells, we compared the laminar distribution patterns of their axons in different cortical areas using anterograde tracing and data available from the MouseLight database of Janelia Research Campus (<http://ml-neuronbrowser.janelia.org/>; Economo et al. 2016; Winnubst et al. 2019). Following the axon distribution analysis, we investigated expression of ER81 (ETS variant transcription factor 1 (ETV1) in human) in L5 IT cells with a projection area identified by retrograde labeling. Our results show that IT cells that preferentially innervate L1, an important target of feedback projections, more frequently express ER81 and project to a greater number of cortical areas than do IT cells with lower preference for L1. Electrophysiological and connective analyses further suggest preferential connectivity among L5 IT cells that share a common innervation pattern. Thus, M2-L5 IT cells are differentiated according to their L1 innervation patterns and these innervation subtypes express ER81 differently, suggesting that they generate diverse feedback signals to lower-order cortical areas.

Materials and methods

Animals

The following mouse lines were used for morphological analysis: ICR (Japan SLC, Inc., Hamamatsu, Japan); Tlx3-Cre PL56 (Tlx3; MGI: 5311700) expressing Cre recombinase (Cre) in L5 IT cells (Gerfen et al. 2013); Rosa-lsl-tdTomato (Ai14; MGI: 3809524) used for Cre reporter (Madisen et al. 2010); VGAT-tdTomato (Line 54) expressing tdTomato in GABAergic cells (Kaneko et al. 2018). The following primers were used for PCR genotyping: 5'-GAAAGATGACACAGAGCCTGTCGGG-3' and 5'-CGGCAAACGGACAGAAGCATT-3' for Tlx3; 5'-CTGTTCTGTACGGCATGG-3' and 5'-GGCATTAAAGCAGCGTATCC-3' for Ai14; 5'-AAGAGATTGCATGGACCTTGG-3', 5'-TCCAGCATATAACAGCACCAG-3' and 5'-TCATCGCTCTGGAGTGAATACC-3' for VGAT-tdTomato. The PCR products were amplified by Premix Taq Hot Start Version (TAKARA

Bio, Inc., Shiga, Japan; RR030A). Red fluorescence was detected through the cephalic skin in tdTomato-expressing mice, which are the progeny of Tlx3 crossed with Ai14 (Tlx3-Ai14). Wistar rats (Charles River Laboratories Japan, Inc., Tsukuba, Japan, or Japan SLC, Inc.) of both sexes were used for morphological analysis. All experiments were conducted in compliance with the guidelines from the Institutional Animal Care and Use Committee of National Institutes of Natural Sciences or Tamagawa University and approved by them.

Retrograde labeling of pyramidal cells

Male and female mice (3–4 weeks old) were anesthetized with a mixture of ketamine (40 mg/kg, intramuscular injection [i.m.]) and xylazine (12 mg/kg, i.m.), or isoflurane (1.0–2.5%), followed with injections of glycerol (0.6 g/kg, intraperitoneal injection [i.p.]) and dexamethasone (3.5 mg/kg, i.p.). In some experiments, 3–4 weeks old male Wistar rats were used and anesthetized in the same manner. After the animals were placed in a stereotaxic apparatus, one of the following retrograde tracers was injected into each mouse cortical region that corresponds to a single area or contains several adjacent areas, as listed in [Supplementary Table 1](#), by pressure injection (PV820 Pneumatic PicoPump; World Precision Instruments, Sarasota, FL, USA) through glass pipettes (tip diameter, 40–60 μm ; approximately 100 nL): Alexa Fluor 647-conjugated cholera toxin subunit B (CTB647; Thermo Fisher Scientific, Waltham, MA, USA; C34778; 0.2% in distilled water or Dulbecco's phosphate-buffered saline); Alexa Fluor 555-conjugated cholera toxin subunit B (CTB555; Thermo Fisher Scientific, C34776; 0.2% in Dulbecco's phosphate-buffered saline); red fluorescent latex microspheres (RetroBeads, Lumafuor); Fast Blue (FB; Dr Illing GmbH and Co. KG, Groß-Umstadt, Hesse, Germany; 2% in distilled water). CTB was also injected into rat cortex ([Supplementary Table 2](#); Ueta et al. 2019). For injection into perirhinal cortex (including ectorhinal area and temporal association area), the pipette was positioned at a 30° lateral inclination (Hirai et al. 2012; Ueta et al. 2013). For retrograde labeling from L1 axonal fibers in mouse and rat, a filter paper ($\sim 1 \text{ mm}^2$) soaked with FB was placed on the pia for ~ 5 min, followed by saline wash (Rubio-Garrido et al. 2009). After a survival period of 4–7 days, the animals were deeply anesthetized with isoflurane and perfused transcardially with a prefixative (250 mM sucrose and 5 mM MgCl_2 in 0.02 M phosphate-buffer (PB) solution, pH ~ 7.4) followed by a fixative (4% paraformaldehyde and 0.2% picric acid in 0.1 M PB solution). The brains were then postfixed in fixative solution for 2 h at room temperature.

Virus injection for axon labeling

After induction of anesthesia as described above, this state was maintained by isoflurane (0.5–2.0%) via inhalation. For Cre-induced fluorescence labeling of somata and axons, AAV5-CAG Double flox synaptophysin-EGFP

vector (Addgene, #73816; Harwell et al. 2012) was prepared using Helper Free Expression System (Cell Biolabs, Inc., San Diego, CA, USA) and injected into M2 (~50 nL; coordinates shown in [Supplementary Table 1](#)). After a survival period of 4 weeks, these mice were perfused with the fixative.

Histological identification of cortical areas, layers, and cell subtypes

The perfusion-fixed brains were cut into 20- μ m-coronal or sagittal sections using a vibratome (Leica Microsystems, Wetzlar, Germany; VT1000S). As primary antibodies, a mouse monoclonal antibody against the neurofilament heavy chain (anti-NF-H; Sigma-Aldrich Co. LLC, St. Louis, MO, USA; N0142; 1:2,000) was used for area identification of M2 (Ueta et al. 2014) and a guinea pig polyclonal antibody against vesicular glutamate transporter type 2 (anti-VGluT2; Merck, Darmstadt, Germany; AB2251; 1:2,000) for layer identification in M2. A mouse monoclonal antibody against vertebrate neuron-specific nuclear protein (anti-NeuN; Merck, MAB377; 1:1,000), a rabbit polyclonal antibody against mouse ER81 (anti-ER81 from Thomas Jessell; 1:20,000; Arber et al. 2000), and a rat monoclonal antibody against chicken ovalbumin upstream promoter transcription factor-interacting protein 2 (anti-Ctip2; Abcam, Cambridge, MA, USA; AB18465; 1:1,000) were used for cell subtype identification. A rabbit polyclonal antibody against GFP (anti-GFP; MBL, Nagoya, Japan; 598; 1:2,000) was used for fluorescence enhancement of synaptophysin-EGFP. Sections were incubated overnight at 4°C with the primary antibodies in 0.05 M Tris-buffered saline (TBS) containing 10% normal goat serum, 2% bovine serum albumin, and 0.5% Triton X-100. Anti-Ctip2 incubation was performed in Can Get Signal immunostain Solution B (TOYOBO, Osaka, Japan; NKB-601) for ~2 h at room temperature. Subsequently, fluorescent secondary antibodies were used: Alexa Fluor 350 for NeuN; 488 or 594 for VGluT2 and ER81; 594 for GFP; 594 or 633 for NF-H; 594 or 647 for Ctip2. The sections were mounted on glass slides and coverslipped with TBS or antifade solution (SlowFade Gold Antifade Mountant, Thermo Fisher Scientific, S36937). Five consecutive sections were used for analysis, in which the third section was used to identify cortical areas and layers, while the remainders were used to count cell bodies.

The labeled neural elements were observed with an epifluorescence microscope (Olympus, Tokyo, Japan; IX-83), and densely labeled synaptophysin-EGFP with a confocal laser scanning microscopy (Olympus, FV1000). Analyses were done using Neurolucida (MBF Bioscience, Williston, VT, USA), IGOR Pro software (WaveMetrics, Inc., Portland, OR, USA), and Image J (NIH). Brightness and contrast of fluorescent images were adjusted using Adobe Photoshop (Adobe Inc., San Jose, CA, USA).

Analysis of anterogradely labeled axons

Synaptophysin-EGFP-labeled puncta (putative axon terminals) were manually counted in L1 and a part of layer

2/3 (L2/3) (the same thickness as L1 from L1/2 border, $128 \pm 26 \mu\text{m}$). The measurement width was increased by 50 μm and at least 100 puncta were counted. Laminar distribution index of L1 and L2/3 was defined as the difference between L1 and L2/3 puncta densities divided by their sum in individual sections.

Morphological analysis using the MouseLight database

Morphological data of L5 PCs in M2 were downloaded from the MouseLight database (<http://ml-neuronbrowser.janelia.org/>, Janelia Research Campus). It was confirmed that each cell was in L5 of M2 in Allen Mouse Common Coordinate Framework (CCFv3) (<http://help.brain-map.org/display/mousebrain/API>) (Kuan et al. 2015; Wang et al. 2020; [Supplementary Table 3](#)). Note that L5 IT cells were defined as L5 cells that project to the contralateral neocortex. Axon distributions were analyzed in following cortical regions: M1 and M2; primary and secondary (supplemental) somatosensory cortex (S1 and S2); auditory cortex (AUD) including dorsal auditory, primary auditory, posterior auditory, and ventral auditory areas; perirhinal cortex and surrounding areas (PER) including perirhinal, ectorhinal, and temporal association areas; visual cortex (VIS) including anterolateral visual, anteromedial visual, lateral visual, primary visual, posterolateral visual, and posteromedial visual areas; orbital cortex (ORB) including orbital area, orbital area lateral, orbital area medial, and orbital area ventrolateral parts.

The axon length was the sum of Euclidean distances between adjacent points. The axon lengths were obtained for individual cortical regions and each layer by referring to the atlas information from AllenID, which includes both ipsi- and contralateral information. When two adjacent points of an axon had different AllenIDs, the distance between them was added to the proximal AllenID. An “endpoint” of axons was defined as a point without further continuation. We calculated standard deviations (SDs) of coordinates between ipsilateral dorsal striatal endpoints in mediolateral, dorsoventral, and anteroposterior axes for individual IT cells. The morphologies were analyzed using custom-made codes in Image J, MATLAB (MathWorks Inc., Natick, MA USA), Ruby (<https://www.ruby-lang.org/en/>), and Microsoft Excel (Microsoft, Redmond, WA, USA).

In vitro electrophysiological recordings

Five- to six-week-old male and female mice were anesthetized with isoflurane (1.0–2.5%), followed by injections of dexamethasone (3.5 mg/kg, i.p.) in glycerol (0.6 g/kg, i.p.), and M2-L5 PCs projecting to the contralateral M2 or ipsilateral PER were retrogradely labeled with CTB647. Three to 14 days after the tracer injection, animals were deeply anesthetized with isoflurane and the brain was quickly removed. The block containing M2 was sliced into 300- μ m-thick oblique horizontal sections (Kawaguchi 1993) with cutting solution: (in mM) 90 N-methyl-d-glucamine, 40 choline Cl, 2 KCl, 1.25

NaH₂PO₄, 1.5 MgCl₂, 0.5 CaCl₂, 26 NaHCO₃, 10 glucose, 4 lactic acid, and 2.5 sodium ascorbate (310 ± 5 mOsm/L, pH 7.4 adjusted with HCl). Slices were immersed in a solution containing (in mM) 125 NaCl, 2.5 KCl, 2 CaCl₂, 1 MgCl₂, 25 NaHCO₃, 1.25 NaH₂PO₄, 10 glucose, and 4 lactic acid (310 ± 5 mOsm/L, pH 7.4). This solution was continuously bubbled with a mixture of 95% O₂ and 5% CO₂. Lactic acid was omitted from the solution used for recordings. Recordings were made in whole-cell mode (Molecular Devices, LLC., San Jose, CA Multiclamp 700B) at 31–32°C. The pipette solution contained (in mM) 130 K-gluconate, 0.2 EGTA, 2 MgCl₂, 2 Na₂ATP, 0.3 NaGTP, and 10 HEPES with 0.75% biocytin. The pH of the solution was adjusted to 7.2–7.3 using KOH, and the osmolarity was 290 ± 5 mOsm/L. Membrane potentials were not corrected for liquid junction potentials. The series resistance of recorded cells was <25 MΩ. Data were analyzed with IGOR Pro software.

Voltage responses to depolarizing and hyperpolarizing current steps (–400 to 600 pA with 50-pA increments, 1-s duration) were obtained. Input resistance (R_i) and time constant were determined with a transient voltage response to hyperpolarizing current injection (–50 pA, 1-s duration; average of 5 times). Voltage sag amplitude was determined by subtracting a steady-state voltage from the negative voltage peak in response to a hyperpolarizing current pulse (–200 pA). Adaptation index was obtained by dividing the frequency-current slope of the last interspike interval with that of the third interval: a larger index means “more slowly adapting”.

The synaptic connections between PCs were investigated by simultaneous recording of two cells within 60 μm in the horizontal plane. Unitary excitatory postsynaptic currents (EPSCs) were recorded at –60 mV by single action potentials elicited by somatic depolarizing current pulses (1-ms duration) in the presynaptic cell (stimulation interval: 5 s). The mean EPSC amplitude and paired-pulse responses were obtained by averaging 20 traces. The paired-pulse ratio at a pulse interval of 100 ms was calculated as the ratio of the mean amplitude of the second EPSC to that of the first EPSC.

After recording, slices were fixed with 4% paraformaldehyde in 0.1 M PB solution for 2 h at room temperature. The fixative was replaced with 30% sucrose in 0.05 M TBS and then the slices were exposed to freeze and thaw 3 times. These were stained by streptavidin conjugated Alexa Fluor 350 (Thermo Fisher Scientific, S11249) and anti-VGluT2 antibody with 5% Triton X-100.

Statistical analysis

Data are presented as mean ± SD. The D’Agostino-Pearson normality test was used to determine if data followed a normal distribution. The difference from the reference was tested by one sample t-test. Morphological differences between two groups were tested by unpaired t-test or paired t-test. The innervation differences among cortical regions were tested by one-way ANOVA and post

hoc Tukey’s multiple comparisons tests. Electrophysiological properties were tested by Mann–Whitney *U* test or Brown-Forsythe one-way ANOVA and post hoc Dunnett’s T3 multiple comparisons tests. Equality of two variances was tested by *F* test. Correlation was tested by Spearman correlation (*R*_s). Statistical examination was performed using GraphPad Prism 8 (GraphPad Software, San Diego, CA, USA). Significance was accepted when *P* < 0.05.

Results

L1 axonal distributions of M2-L5 IT cells dependent on their innervated cortical area

M2 innervates L1 of other cortical areas (Ueta et al. 2013), and M2-L5 IT cells locally send axon collaterals to L1 (Hirai et al. 2012). Therefore, we investigated how L5 IT cells contribute to L1 innervation in areas other than M2. For selective labeling of L5 IT cells, we utilized Tlx3-Cre PL56 mouse line (Gerfen et al. 2013). L5 is divided into L5a (upper) and L5b (lower): L5b is more positive for VGluT2, which is a marker of axonal terminals from thalamus, than L5a (Fig. 1A; Morishima et al. 2011). Cre-expressing cells in Tlx3 mice (Tlx3 cells), labeled fluorescently by crossbreeding with Ai14 mice (Rosa-lsl-tdTomato), were distributed predominantly in L5a (Fig. 1A “Ai14”). Tlx3 cells labeled fluorescently by M2 local virus injection were also found more in L5a (Fig. 1A “AAV”). CPn cells of PT type were labeled retrogradely from the pons. One out of 196 L5a CPn cells and none of 358 L5b CPn cells overlapped with Tlx3 cells (3 Tlx3-Ai14 mice). About 250 out of 633 L5a contralateral M2-projecting (cM2p) cells and 97 of 445 L5b cM2p cells overlapped with Tlx3 cells (3 Tlx3-Ai14 mice). Thus, Tlx3 cells are a subpopulation of IT cells.

To investigate the specificity of L1 innervation of M2-L5 IT cells, we compared the axon terminal densities of Tlx3 cells between L1 and L2/3 in each cortical region (that corresponds to a single area or contains several adjacent areas in this paper). For fluorescent axon labeling, synaptophysin-EGFP, more preferentially distributed in axons/somata than dendrites, was introduced into Tlx3 cells in M2 by using an AAV vector (Harwell et al. 2012). The fluorescent puncta were considered as putative synaptic boutons of axons (Fig. 1B). Differences in L1 and L2/3 innervation were assessed by quantifying L1 preference index as follows: the difference in the density of fluorescent puncta between L1 and L2/3 divided by their sum (+1: distribution only in L1; –1: only in L2/3). Innervation patterns were analyzed where labeled axons were most densely distributed within each target cortical region. M2-Tlx3 cells uniformly innervated L1 and L2/3 in local M2 (index = –0.0022 ± 0.027, 3 mice, *P* = 0.90, one sample t-test, hypothetical value = 0), but preferentially L1 in ipsilateral M1 (index = 0.53 ± 0.15; *P* = 0.024), ipsilateral S1 (index = 0.60 ± 0.15; *P* = 0.020), ipsilateral AUD (index = 0.66 ± 0.16; *P* = 0.019), and ipsilateral PER (index = 0.32 ± 0.11; *P* = 0.038; Fig. 1C). L1 preferences in the contralateral cortical region were not different

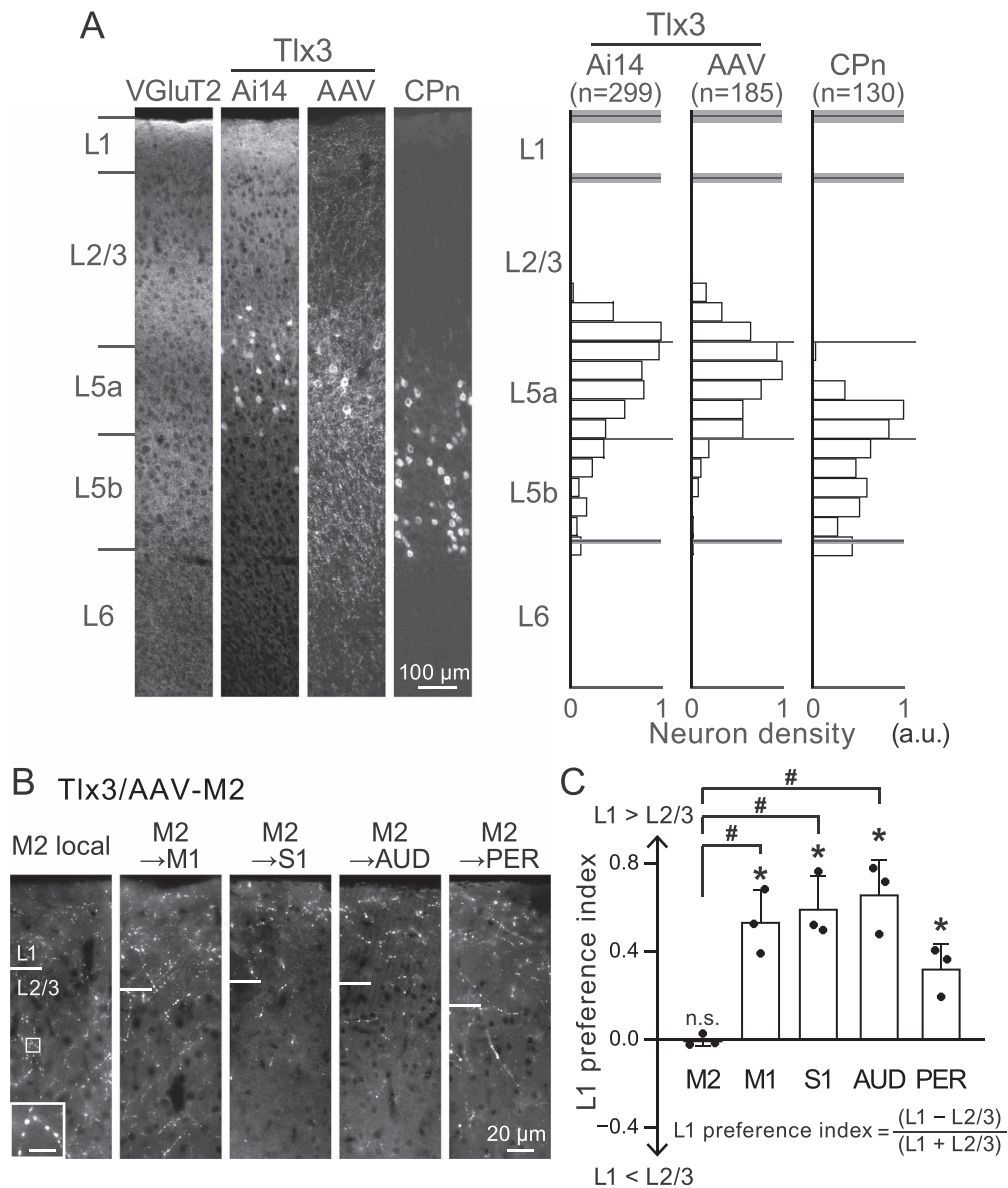


Fig. 1. Axonal distributions of M2 Tlx3 cells of L5 IT subtype. **A**) Laminar distributions of somata of Tlx3 cells in M2. VGlut2, immunoreactivity used for layer identification; Tlx3, fluorescence detection by crossing with the reporter line (Ai14); that by local virus injection (AAV); CPn cells labeled with a retrograde tracer (CTB). Sections were 200 μ m wide and 20 μ m thick. Right graph, distribution of the fluorescently labeled somata (Ai14 and CPn, 3 mice; AAV, 2 mice). Cortical thickness was normalized by L5a thickness; depth intervals, one-fifth of L5a thickness; layer border, black line represents mean and gray bar indicates SD. (n), number of cells. **B**) Axonal distributions of M2 Tlx3 cells in M2 local and ipsilateral cortical regions. Axon fibers were labeled by Cre-dependent induction of synaptophysin-EGFP (AAV5-CAG Double flox synaptophysin-EGFP), which accumulated preferentially at the axon terminals (seen as puncta). Inset in “M2 local”, enlargement of rectangle in L2/3; scale bar, 5 μ m. M2, secondary motor cortex; M1, primary motor cortex; S1, primary somatosensory cortex; AUD, auditory cortex including dorsal auditory, primary auditory, posterior auditory, and ventral auditory areas; PER, perirhinal cortex and surrounding areas including perirhinal, ectorhinal, and temporal association areas. **C**) Comparisons of L1 and L2/3 distribution of M2 Tlx3 cells’ axon puncta in different cortical regions. The difference between L1 and L2/3 was quantified by laminar distribution index of puncta density: positive for L1 preference and negative for L2/3 preference. Data, mean + SD (3 mice for each). * $P < 0.05$ (one sample t-test, hypothetical value=0), # $P < 0.05$ (ordinary one-way ANOVA, $P < 0.001$; post hoc Tukey’s multiple comparisons test).

from those in the same region on the ipsilateral side (contra-M2, index = -0.049 ± 0.055 , $P = 0.33$; contra-M1, index = 0.35 ± 0.14 , $P = 0.23$; contra-PER, index = 0.38 ± 0.12 , $P = 0.68$, paired t-test). The L1 preference of M2-Tlx3 cells was higher in M1, S1, and AUD than in M2 ($P < 0.001$, ordinary one-way ANOVA test; M2 vs. M1, $P = 0.0030$; M2 vs. S1, $P = 0.0014$; M2 vs. AUD, $P < 0.001$; M2 vs. PER, $P = 0.065$, post hoc Tukey’s multiple comparisons test). These results suggest that L1 innervation by populations

of M2-L5 IT cells differs between M2 itself and other cortical areas.

Correlation between L1 innervation preference and projection patterns in L5 IT cells

The above observations suggest that M2-L5 IT cells may innervate L1 in other cortical areas more than in M2 locally or be composed of subtypes with different L1 innervation strengths. To distinguish between these two

possibilities, we investigated the relationship between the cortical areas and layers innervated by individual M2-L5 IT cells whose axon collaterals have been morphologically reconstructed, available from MouseLight project (Janelia Research Campus; <http://ml-neuronbrowser.janelia.org/>; [Economio et al. 2016](#); [Winnubst et al. 2019](#)).

In this database, we analyzed PCs belonging to M2-L5 defined in the Allen atlas ([Supplementary Table 3](#); [Kuan et al. 2015](#); [Wang et al. 2020](#)). All M2-L5 PCs other than PT cells projecting to the pons sent axons to the contralateral neocortex (IT cells; $n=39$). We calculated the axonal length in individual target cortical regions and layers. Among the 39 IT cells, 34 cells actually innervated L1. PC axons innervate L1 through L2/3. L1/2/3 axon length of L1-innervating IT cells was $40,031 \pm 41,192 \mu\text{m}$ (34 cells; range: 1,308–174,888 μm). We assumed that 37 IT cells with L1/2/3 axon length longer than 1,308 μm could innervate L1. We further analyzed these 37 cells (L5 IT cells with potential L1 innervation, including 3 cells without L1 innervation; [Supplementary Table 3](#)).

M2-L5 IT cells exhibited variable density of innervation in L1 ([Fig. 2A](#) left and right; arrow and arrowhead in B and C, respectively). To quantify layer preferences in the innervation of individual M2 cells, we calculated the ratio of axon length in L1 and L5/6a to total axon length in L1/2/3/4/5/6a (L1 axon ratio or L5/6a axon ratio, respectively). Ipsi- and contralateral axon ratios were well correlated ([Supplementary Fig. 1A](#); L1 axon ratio: $R_s=0.60$, $P < 0.001$; L5/6a axon ratio: $R_s=0.47$, $P=0.0032$; Spearman correlation test), which suggests that the layer preference in innervation is bilaterally maintained. Both L1 and L5/6a axon ratios including both hemispheres were independent of the total axon length in bilateral neocortex (L1: $P=0.50$; L5/6a: $P=0.75$; [Fig. 2B](#)). The L1 and L5/6a axon ratios in bilateral neocortex excluding M2 were correlated with those in M2 ([Fig. 2C](#)). This suggests that the laminar distribution of L5 IT cell axons in the target region reflects that in their M2 origin and that diversity of L1 innervation preferences between M2-L5 IT cells explain interareal variation in L1 distribution of anterogradely labeled axons from a population of M2-L5 IT cells ([Fig. 1C](#)).

Since the M2-L5 IT cells sent axons to diverse cortical regions, we investigated the relationship between L1 innervation preference (L1 axon ratio in neocortex) and axon length in respective cortical regions (bilateral axon length in M2, M1, S1, S2, AUD, PER, VIS, and ORB) in the MouseLight database ([Fig. 3A](#): axon length in each region of 37 cells, tentatively divided into 4 groups according to the L1 axon ratio for clarity). Innervation variability between target cortical regions was represented by coefficient of variance ($CV=SD/\text{mean}$) of normalized axon length (1: maximum length of each cortical area) in 8 cortical regions (M2, M1, S1, S2, AUD, PER, VIS, and ORB). The cells with smaller CV innervate the cortical regions more uniformly, and those with larger CV project to a smaller number of regions. The inter-regional CV was negatively correlated with L1 axon

ratio ($R_s=-0.37$, $P=0.024$; [Fig. 3B](#) top), but independent of L5/6a axon ratio ($R_s=0.22$, $P=0.19$; [Fig. 3B](#) bottom). Ipsi- and contralateral inter-regional CV were well correlated ([Supplementary Fig. 1B](#); L1 axon ratio: $R_s=0.37$, $P=0.025$). The cells with lower L1 axon ratio were larger in CV and sent axonal projections to limited regions, such as M1 ([Fig. 3A](#) left graphs). The cells with higher L1 axon ratio were smaller in inter-regional CV and diverse in target region pattern ([Fig. 3A](#) right graphs). This suggests that L1-preferring IT cells innervate more cortical areas than IT cells with lower L1 preference.

Next, we examined whether the density of innervation in certain region(s) was associated with L1 axon preference. The L1 axon ratio of M2-L5 IT cells was independent of the axon length in M1 ($R_s=-0.14$, $P=0.40$) but was correlated with the axon length in AUD ($R_s=0.41$, $P=0.012$) and PER ($R_s=0.51$, $P=0.0012$; [Fig. 3C](#)). The correlation between L1 axon ratio and axon length was similar between individual ipsi- and contralateral regions ([Supplementary Fig. 1C](#)). This analysis confirmed that M2-L5 IT cells are composed of subtypes with different L1 innervation preferences that are associated with the projection region. This indicates that L1-preferring IT cells target more diverse regions, including AUD and PER.

Relation between corticostriatal and corticocortical innervations of L5 IT cells

The other main target of L5 IT cells is the striatum of the basal ganglia. Since basal ganglia output is transmitted through the thalamus to cortical L1, we conceived the possibility that the L1 innervation pattern might be related to the striatal projection pattern because M2 PCs have various spatial spreads of striatal axons, revealed by analysis of MouseLight database ([Fig. 4A](#); [Morita et al. 2019](#)). Total axon length in bilateral striatum was independent of that in bilateral neocortex ($R_s=0.22$, $P=0.20$; [Fig. 4B](#)). All L5 IT cells innervated the dorsal striatum (dStr), while some of them also innervated the ventral striatum (vStr; [Fig. 4A](#)). Both axon lengths in dStr and that in vStr were well correlated with the L1 axon ratio (dStr: $R_s=0.43$, $P=0.0083$; vStr: $R_s=0.53$, $P < 0.001$; [Fig. 3C](#) right). The L1 axon ratio was correlated with the ratio of vStr axon length to total striatal axon length ($R_s=0.53$, $P < 0.001$; [Fig. 4C](#)). The data suggest that L1-preferring IT cells have greater total length of striatal axons and are more likely to innervate the vStr than L1-nonpreferring IT cells.

Since the striatum, especially dStr, is a large nucleus, the spatial pattern of innervation is important for corticostriatal function ([Kincaid et al. 1998](#); [Zheng and Wilson 2002](#); [Hooks et al. 2018](#)). To quantify the spatial extent of the axon collaterals within the dStr, we calculated the SDs of endpoint coordinates for each M2-L5 IT cell (endpoint SDs) in ipsilateral dStr ([Morita et al. 2019](#)). The L1 axon ratio was correlated with the endpoint SDs in ipsilateral dStr (mediolateral: $R_s=0.39$, $P=0.0020$; dorsoventral: $R_s=0.66$, $P < 0.001$; anteroposterior: $R_s=0.56$, $P < 0.001$; [Fig. 4D](#)). Larger endpoint SD of

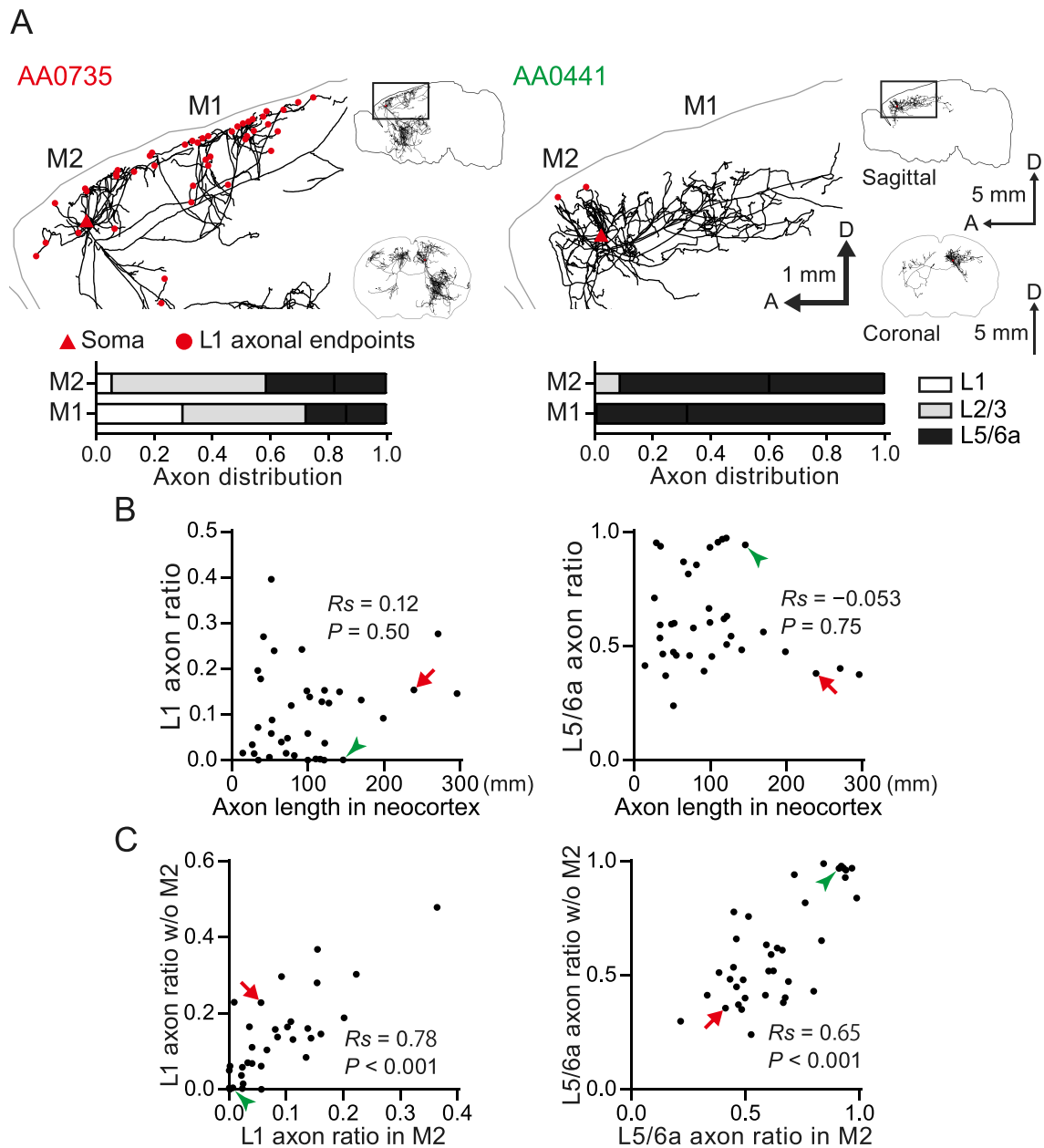


Fig. 2. Heterogeneity in laminar axonal innervation of M2 L5 IT cells obtained from the MouseLight database. A) Two examples of M2-L5 IT cells from the MouseLight database. AA0735, cell with dense axon arborizations in L1; AA0441, with few axon collaterals in L1. Red triangle, soma; red circles, axon endpoints (points without further continuation) in L1. Right, ipsi-hemisphere sagittal projections (top) and coronal projections (bottom) are presented; the rectangle area was enlarged. A, anterior; D, dorsal. Bar graphs, laminar distributions of axon length normalized to the total length in L1/2/3/5/6a of bilateral M2 and M1, respectively. AA0735, 12 endpoints in ipsilateral M2 and 11 endpoints in iM1; AA0441, 2 endpoints in iM2 and 0 endpoints in iM1. B) Relationship of axon distribution ratio in L1 or L5/6a to total axon length in L1/2/3/4/5/6a of bilateral neocortex (37 cells). R_s and P , Spearman correlation test. Red arrow, cell on the left in (A); green arrowhead, cell on the right in (A). C) Relationship of the L1 or L5/6a axon ratio in bilateral neocortex excluding M2 to that in bilateral M2.

L5 IT cells with L1 preferential innervation suggests that they project to more heterogeneous regions in the dStr.

The close relationship between the L1 axon ratio of L5 IT cells and their cortical projection regions including AUD and PER indicates that the striatal innervation style is also associated with the target cortical region. The axon lengths in AUD and PER were correlated with endpoint SDs in ipsi-dStr, as was the L1 axon ratios (AUD: $R_s = 0.33$, $P = 0.054$ in mediolateral, $R_s = 0.36$, $P = 0.034$ in dorsoventral, $R_s = 0.29$, $P = 0.090$ in anteroposterior; PER:

$R_s = 0.49$, $P = 0.0030$ in mediolateral, $R_s = 0.39$, $P = 0.021$ in dorsoventral, $R_s = 0.43$, $P = 0.0095$ in anteroposterior; Fig. 4E). Thus L1-preferring IT cells of M2-L5 innervate AUD and PER more densely and also more heterogeneous regions in the striatum than nonpreferring cells.

Next, we further confirmed whether L1-preferring IT cells innervate a larger volume of the striatum than nonpreferring cells. Since the spiny projection neurons of striatum extend spines up to $2 \mu\text{m}$ (Wilson et al. 1983), we considered that corticostriatal axons could make

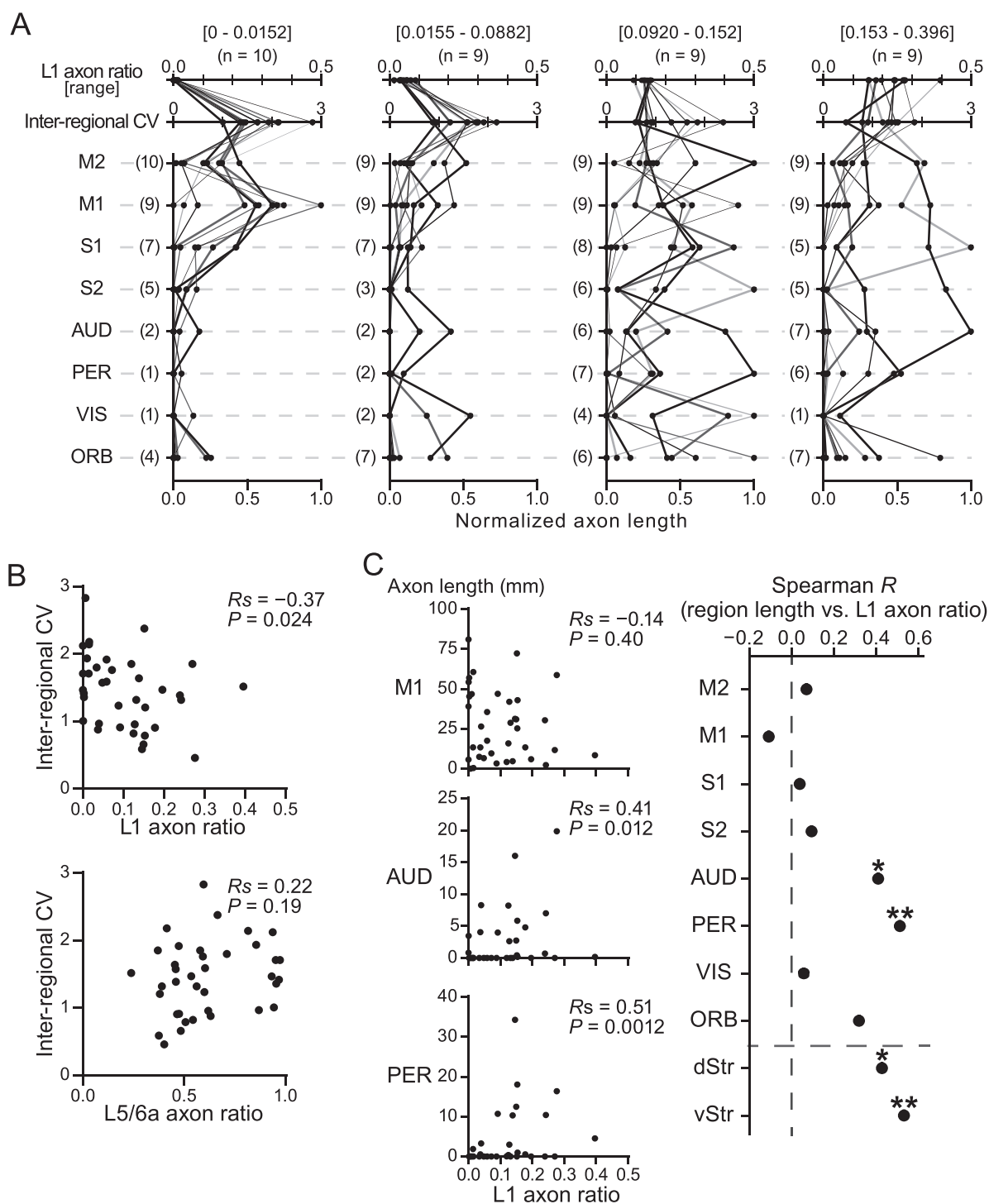


Fig. 3. Correlation between L1-inervation preference and corticocortical projection pattern. A) Relationship of the axon length in respective innervated regions to L1 axon ratio in neocortex. The L1 axon ratio and inter-regional CV (SD/mean of axon lengths in 8 innervated cortical regions) are displayed at the top. The axon length in each region was normalized to the maximum there. Individual M2-L5 IT cells (MouseLight database) are connected by lines. The same cells are connected by distinct grayscale lines to easily distinguish them. For clarity, the M2-L5 IT cells were tentatively divided into 4 groups according to the L1 axon ratio. S2, secondary (supplemental) somatosensory cortex; VIS, visual cortex including anterolateral, anteromedial, lateral, primary, posterolateral, and posteromedial visual areas; ORB, orbital cortex including orbital area, orbital area lateral, medial, and ventrolateral parts. (n), (number of projecting cells). B) Relation of the inter-regional CV to the L1 or L5/L6a axon ratio in neocortex (37 cells). C) Relation of axon length in each innervated region to the L1 axon ratio in neocortex. No correlation was found in M1, but positive correlation was observed in AUD and PER. The coefficient of correlation in each region is shown in the right figure. * $P < 0.05$; ** $P < 0.005$ (Spearman correlation test). dStr, dorsal striatum. vStr, ventral striatum.

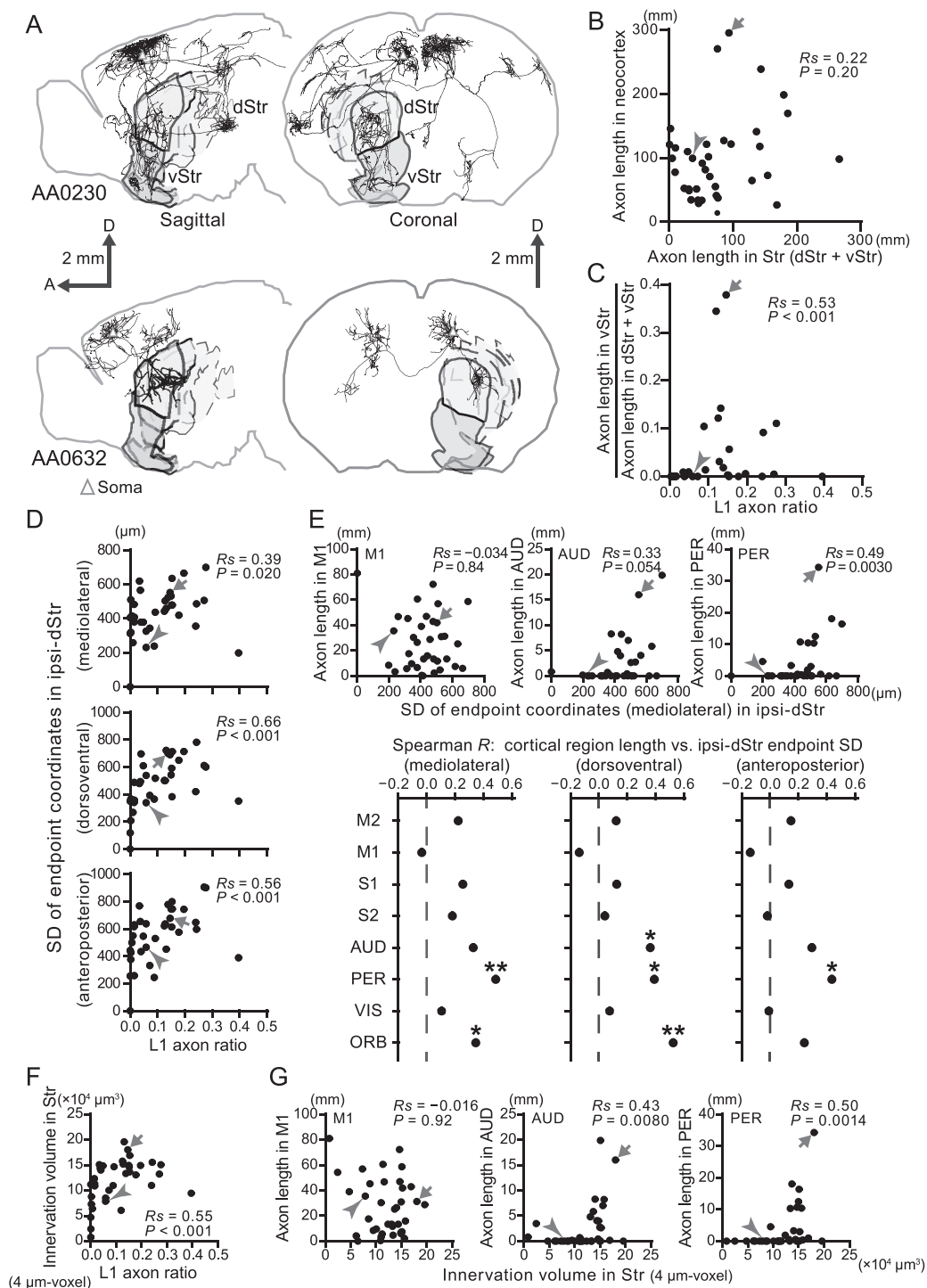


Fig. 4. Corticostriatal innervation patterns of M2-L5 IT cells. A) Two examples of striatum projecting M2-L5 IT cells. Top, cell with dense axon arborizations in vStr; bottom, with no axon collaterals into vStr. Triangle, soma. A, anterior; D, dorsal. B) Relationship between the axon lengths in whole Str and in neocortex. Arrow, cell on the top in (A); arrowhead, cell at the bottom in (A). Cell number = 37. C) Relationship between the ratio of axon length in vStr to entire Str and the L1 axon ratio. D) Relation of the SD of axonal endpoint coordinates (mediolateral, dorsoventral, and anteroposterior) in ipsilateral dStr to the L1 axon ratio. Cell number = 35. E) Relation of axon length in each cortical region to the SD of endpoints coordinates. The SD of mediolateral endpoint coordinates did not correlate with axon length in M1 but positively correlate with axon length in AUD and PER, shown above. The coefficient of correlation of axon length in each cortical region with SD of mediolateral, dorsoventral, and anteroposterior coordinates is shown below. * $P < 0.05$; ** $P < 0.005$ (Spearman correlation test). F) Relation of striatal innervation volume (4 μm -voxel) with L1 axon ratio of M2-L5 corticostriatal cells. G) Relation of axon length in each cortical region with striatal innervation volume of the corticostriatal cells.

synapses with their dendrites within a cube with a side length of 4 μm (4- μm voxel). The innervation volume of L5 IT cells was calculated from the number of 4- μm voxels in which their axons are distributed. The

innervation volume was well correlated with endpoint SDs in ipsi-dStr (Supplementary Fig. 2; $R_s = 0.64$, $P < 0.001$ in mediolateral, $R_s = 0.76$, $P < 0.001$ in dorsoventral, $R_s = 0.57$, $P < 0.001$ in anteroposterior). The innervation

volume was correlated with the L1 axon ratio (Fig. 4F). The innervation volume in ipsi-dStr was correlated with the axon length in AUD and PER (Fig. 4G; AUD: $R_s = 0.43$, $P = 0.008$; PER: $R_s = 0.50$, $P = 0.0014$), but not with the axon length in M1 ($R_s = -0.016$, $P = 0.92$).

ER81 as a candidate molecular marker for L1-preferring IT cells

L5 PCs have heterogeneous gene expression patterns (Molyneaux et al. 2009; Tasic et al. 2018). We explored the possibility that the difference in cortical innervation between M2-L5 IT cells is related to that in molecular expression. Among the molecules found in L5 PCs, a transcription factor *Ctip2* is expressed rarely in IT cells but frequently in PT type (Arlotta et al. 2005; Ueta et al. 2014), whereas another transcription factor ER81 (ETV1) is expressed in both IT and PT cells (Yoneshima et al. 2006; Harb et al. 2016).

In mouse M2-L5, *Ctip2*-positive cells were found more in L5b, but ER81 more in L5a (Fig. 5A). ER81 expression in cM2p cells was found more in L5a (65.3%, 330 out of 505 cells; Fig. 5B) than in L5b (3.5%, 20 out of 577 cells). Furthermore, ER81 was expressed in *Tlx3* cells (73.5%, 482 out of 656 cells, 3 mice) that were distributed mostly in L5a.

Both L5a and L5b contained corticocortical cells. The L5a and L5b distribution of corticocortical cells was dependent on the target region (Fig. 5C). Corticocortical cells that projected to ipsilateral M1 were distributed in both L5a and L5b of mouse M2 (soma distribution index = 0.21 ± 0.49 , $P = 0.45$; one sample t-test, hypothetical value = 0), but those to S1, AUD, and PER were much more distributed in L5a (index = 0.56 ± 0.34 , $P = 0.020$; index = 0.46 ± 0.092 , $P = 0.013$; index = 0.77 ± 0.20 , $P = 0.021$, respectively). The cM2p cells were found more in L5b than in L5a (index = -0.19 ± 0.029 , $P = 0.0074$). This suggests that ipsilateral corticocortical IT cells are more distributed in L5a than in L5b.

Ctip2 was a specific marker for PT cells in L5a: *Ctip2* was expressed in all CPn cells (PT type) of L5a (196 cells, 3 mice) and of L5b (358 cells), but in a few of IT-type cM2p cells of L5a (1.5%; 3 out of 194 cells, 3 mice) and more than half of L5b (62.3%; 142 out of 228 cells). In *Tlx3* cells (IT type), only 1.3% of the population in L5a was *Ctip2*-positive (4 out of 309 cells, 3 mice) while 24.7% of the population in L5b was found to be positive (18 out of 73 cells). These indicated that *Ctip2* could be used as a molecular marker for PT cells in L5a. Proportion of *Ctip2* cells in L5a was 31.8% (54 out of 170 cells) in ipsilateral M1-projecting (iM1p) cells, 22.9% (61 out of 266 cells) in S1-projecting (iS1p) cells, 6.7% (30 out of 415) in AUD-projecting (iAUDp) cells, and 1.5% (3 out of 198 cells) in PER-projecting (iPERp) cells. Thus, M2-L5a corticocortical cells contain both IT and PT types, and IT cells participate more in the projections to AUD and PER (Ueta et al. 2013).

Considering that L5b IT cells were mostly negative for ER81 (Fig. 5B) and rarely projected to AUD and PER (Fig. 5C), we hypothesized that ER81 expression is shared

more among L1-preferring L5a IT cells projecting to AUD and PER than nonpreferring cells. To test this hypothesis, first, we further confirmed that L5a IT cells contain both ER81-positive and -negative cells. For this purpose, we identified L5a IT cells as NeuN-immunopositive and *Ctip2*-immunonegative cells among nonfluorescent cells of VGAT-tdTomato mice (Fig. 5D; Kaneko et al. 2018). In L5a, IT cells accounted for 63.0% of PCs ($n = 1126$, 3 mice). ER81 was expressed in 57.5% of L5a IT cells ($n = 709$, 3 mice; Fig. 5E) and in 80.3% of L5a PT cells ($n = 417$, 3 mice). The division of L5a IT cells into two major subgroups depending on ER81 expression suggests a possible association with corticocortical innervation pattern.

To identify target cortical areas of L5a ER81-positive cells, a retrograde tracer (CTB) was injected into L1 to L6 in a layer-nonspecific manner (Fig. 6A "CTB"). ER81 was expressed in most of L5a IT cells (negative for *Ctip2*) projecting to iPER ($93.4 \pm 0.7\%$, $n = 236$, 3 mice), but partially in those projecting to iM1 ($65.9 \pm 1.4\%$, $n = 113$, 3 mice) and to iS1 ($63.6 \pm 2.3\%$, $n = 205$, 3 mice; Fig. 6B top, Fig. 6C white bars). Layer-nonspecific injection of another retrograde tracer (FB) into S1 yielded similar results ($68.6 \pm 3.0\%$, $n = 352$, 3 mice; data not shown). The expression rate was intermediate in iAUDp cells ($80.9 \pm 4.6\%$, $n = 384$, 3 mice). Thus, ER81-negative IT cells projected mostly to the proximal areas such as M1 and S1.

ER81 is expressed more in L5 IT cells that project to PER and AUD than those to M1 and S1, and that the former IT cells innervate L1 more than the latter ones (Fig. 3). These suggested that L1-preferring IT cells express ER81 more than the nonpreferring cells regardless of target area. To confirm this point, a retrograde tracer FB was applied to the cortical surface to label axons around L1 of M1, S1, and AUD (Fig. 6A "FB"). In contrast to the layer-nonspecific injection, M2 IT cells labeled by L1 tracer application in these cortical regions (*cortex*-L1p: layer1 projecting) were mostly positive for ER81 (iM1-L1p: $92.5 \pm 6.5\%$, $n = 95$, 3 mice; iS1-L1p: $90.9 \pm 1.2\%$, $n = 219$, 3 mice; iAUD-L1p: $92.0 \pm 2.0\%$, $n = 532$, 3 mice; Fig. 6B bottom, 6C gray bars). The proportion of ER81-positive cells labeled by the L1 tracer application was like that by layer-nonspecific application in PER. These results suggest that M2-L5a IT cells are composed of diverse neurons with a correlation between ER81 expression, cortical projection areas, and L1 innervation patterns.

Furthermore, we confirmed that L1 preference diversity of L5 IT cells was also conserved in the contralateral hemisphere projection. ER81-positive cells were found more in L5a cells labeled by tracer application to L1 of cM2 (cM2-L1p: $88.9 \pm 1.8\%$, $n = 326$, 3 mice; Fig. 6D) than L5a cells labeled by layer-nonspecific injection there (cM2p: $66.3 \pm 3.9\%$, $n = 505$, 3 mice). These results suggest that L5a IT cells that innervate L1 of cM2 express ER81 more strongly. They also suggest that L1-preferring IT cells are more often found in iPERp cells than iM1p cells. This was confirmed by examining the relationship of L5a cM2-L1p cells labeled by FB application with iPERp and

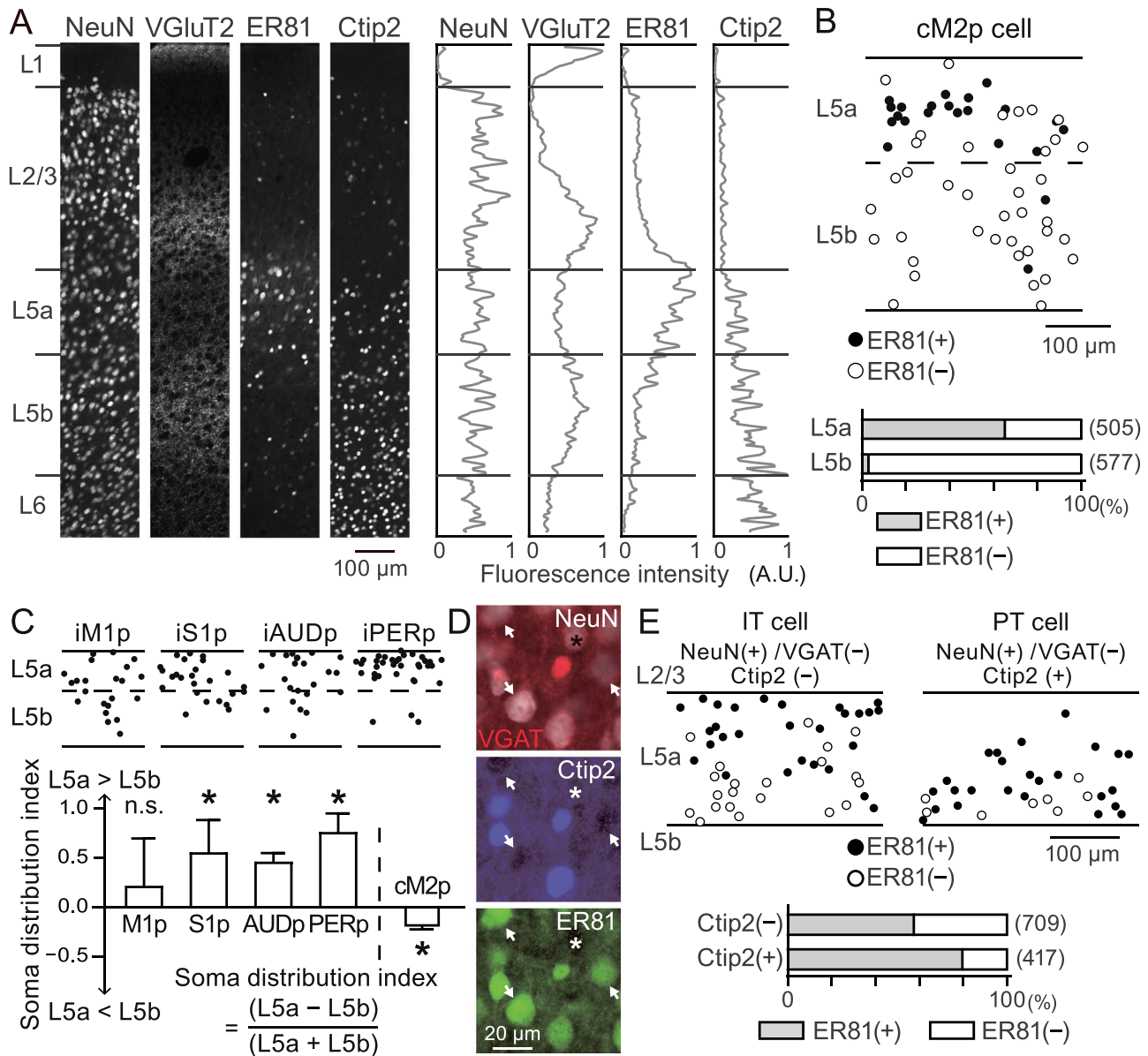


Fig. 5. ER81 expression in a subpopulation of IT cells in L5a. **A)** Laminar distribution of ER81- and Ctip2-positive neurons. The layers were identified by immunofluorescence for NeuN and VGlut2. Sections: 200 μ m wide and 20 μ m thick. Right, fluorescence intensity was quantified every 5- μ m depth and normalized by the maximum value. **B)** ER81 expression in contralateral M2-projecting (cM2p) cells. Top, cell distributions in L5. Filled circle, positive for ER81; open circle, negative for ER81. Bottom, proportion of ER81-positive cells in L5a and L5b cM2p cells (3 mice). (n), number of cells. **C)** Distribution of corticocortical cells in L5a and L5b, labeled retrogradely from other regions. Top: filled circle, retrogradely labeled neuron; laminar depth, normalized by L5a thickness. Bottom: soma distribution index between L5a and L5b (positive, more cells in L5a); data, mean \pm SD (4 mice for iM1p and iS1p, 3 mice for iAUDp, iPERp, and cM2p); * $P < 0.05$ (one sample t-test, hypothetical value = 0). iM1p, iS1p, iAUDp, and iPERp: cells projecting to ipsilateral M1, S1, AUD, and PER, respectively. **D)** ER81 expression heterogeneity in L5a IT cells. L5a IT cells were identified by NeuN expression (in white; top) without VGAT-tdTomato (in red) and Ctip2 expression (in blue; middle). Fluorescence, represented by pseudocolors. Arrows, ER81-positive IT cells; asterisk, ER81-negative IT cells. **E)** ER81 expression in IT and PT cells in M2-L5a, which were negative and positive for Ctip2, respectively. Top, cell distributions in L5a. Bottom, proportion of ER81-positive cells in Ctip2-negative IT and -positive PT cells (3 mice). (n), number of cells.

iM1p cells without Ctip2 expression in the same mice (Supplementary Fig. 3). Proportion of FB-labeled cell in iPERp cells was larger than that in iM1p cells in individual animals ($58.5 \pm 5.3\%$ for iPERp cells and $35.6 \pm 9.1\%$ for iM1p cells, 3 mice; $P = 0.019$, paired t-test).

ER81 expression in L5a IT cells of rat M2

We confirmed the correlation of ER81 expression with L1 innervation preference and with iPER projection in rat M2 (Supplementary Fig. 4A). ER81 expression in L5a cM2p

cells was similar between mice ($66.3 \pm 3.9\%$; Fig. 6D) and rats ($65.1 \pm 3.9\%$; $n = 292$, 3 rats; Supplementary Fig. 4B), and its expression in L5a cM2-L1p cells was also similar between mice ($88.9 \pm 1.8\%$) and rats ($87.9 \pm 3.4\%$, $n = 412$, 3 rats). ER81 expression was not detected in most L5b cM2p cells in mice ($3.4 \pm 0.4\%$; Fig. 5B) but was detected in some rat cells ($33.5 \pm 9.4\%$, $n = 635$; Supplementary Fig. 4C). In L5b of rats, ER81 was similarly expressed in both cM2p and cM2-L1p cells ($36.7 \pm 2.7\%$, $n = 392$; Supplementary Fig. 3C). This indicates that ER81

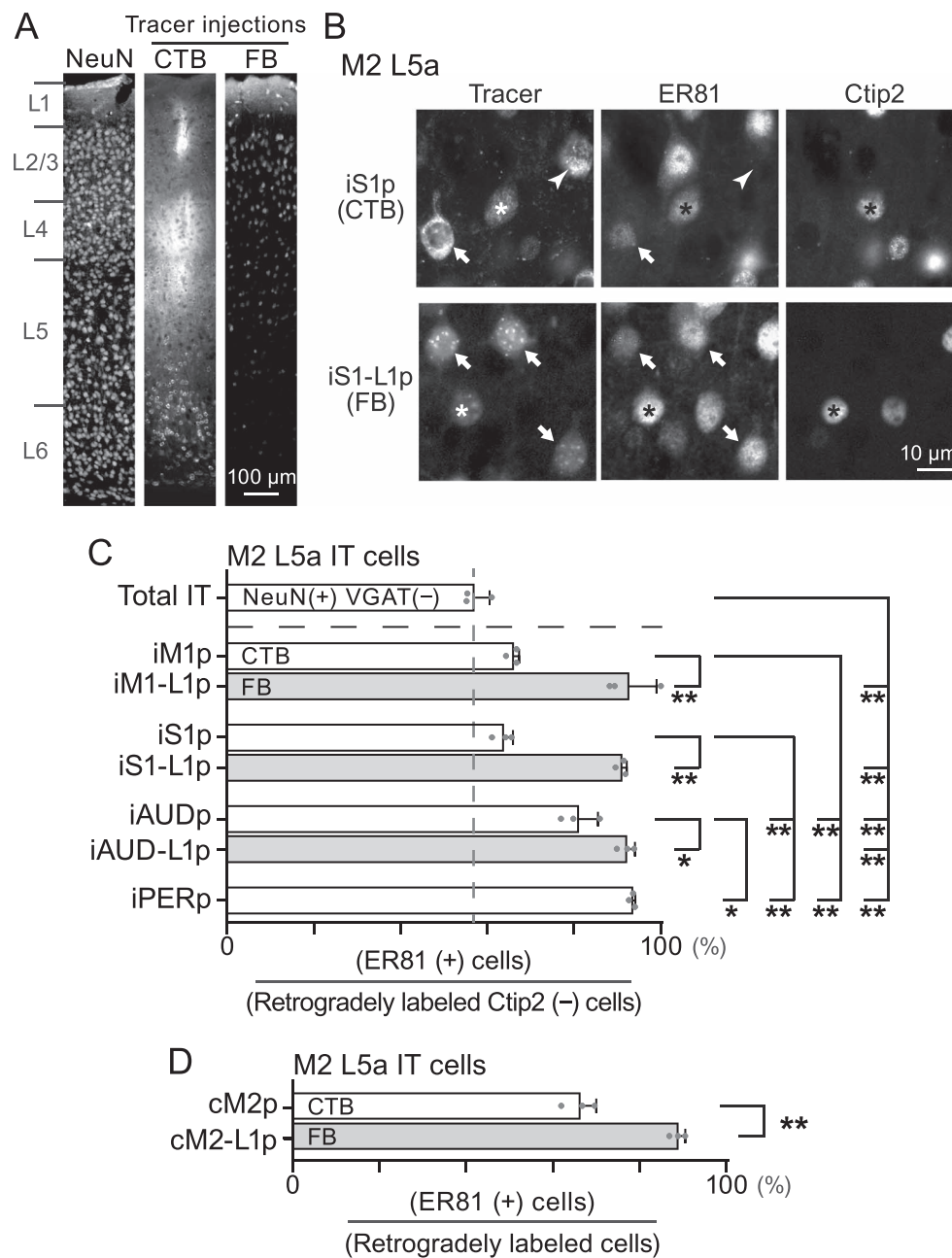


Fig. 6. ER81 expression in M2-L5a is related to L1 innervation and corticocortical projection pattern. A) Two kinds of retrograde labeling: CTB injection across all layers and FB application onto the cortical surface (L1p: L1 projecting). For the CTB injection photograph, three images were overlaid. B) ER81 expression in iS1p and iS1-L1p cells. Top: iS1p IT cells (negative for Ctip2; shown in right) were positive (arrow) or negative (arrowhead) for ER81. Asterisk, cell positive for both Ctip2 and ER81. Bottom: iS1-L1p IT cells (negative for Ctip2; shown right) were positive for ER81 (arrows). C) Proportion of ER81 cells in ipsilateral corticocortical L5a IT cells. Total IT, the proportion of ER81 cells in L5a IT cells (the same data set as in Fig. 5E). The proportion was higher in cells projecting to iAUD and iPER than those to iM1 and iS1 and higher in iM1-L1p, iS1-L1p, and iAUD-L1p cells than in iM1p, iS1p, and iAUDp cells, respectively (3 mice for each). * $P < 0.05$ ** $P < 0.005$ (ordinary one-way ANOVA, $P < 0.001$; post hoc Tukey's multiple comparisons test). D) Proportion of ER81-positive cells in L5a cM2p IT cells. The proportion was higher in cM2-L1p cells than in cM2p cells (3 mice for each). ** $P < 0.005$ (unpaired t-test).

expression in L5a is associated with L1 innervation preference in both mice and rats.

In rat M2, L5 iPERp cells were more distributed in L5a than in L5b. L5a iPERp cells were mostly positive for ER81 ($91.1 \pm 1.2\%$, $n = 526$; Supplementary Fig. 4A and B). Thus, L5a iPERp cells were positive for ER81 in both species. L5b iPERp cells were also almost positive for ER81 in rats ($89.7 \pm 5.8\%$, $n = 118$). ER81 expression in L5a iM1p cells ($66.5 \pm 0.6\%$, $n = 179$) was similar to the expression in L5a cM2p cells. These suggest that ER81 expression in L5a IT

cells is related to L1 innervation and also to perirhinal projection in both mice and rats.

Electrophysiological and connection properties of L5 IT cells

The results so far indicate that in L5a, cM2p cells positive for ER81 project to diverse cortical areas including the iPER, but cM2p cells negative for ER81 innervate only a few areas, especially M1, and that L5b houses more cM2p cells negative for ER81, some of which project to

M1. Next, we determined whether L5 IT cells with different cortical projection and molecular expression also have different electrophysiological properties. Since we already have specific electrophysiological data for some L5 projection subtypes of PCs in juvenile rats, recorded in unpublished and published experiments (Hirai et al. 2012; Ueta et al. 2014), so we first compared the L5 PC subtypes in juvenile rat M2.

In rat M2, the physiological parameters were different between L5a iPERp, L5a cM2p, and L5b cM2p cells (Supplementary Table 4). The firing adaptation was faster and time constant smaller in L5a iPERp cells than L5b cM2p cells. The input resistance was lower and voltage sag smaller in L5a iPERp cells than in L5a and L5b cM2p cells (Supplementary Table 4). L5a and L5b PT cells have different output targets: L5 corticothalamic (CTh) cells are distributed in both L5a and L5b (more in L5a), while corticospinal (CSp) cells are predominantly distributed in L5b (Ueta et al. 2013). The physiological parameters were more comparable between the two PT cell groups than IT cell groups in rats (Supplementary Table 4; Hattox and Nelson 2007; Dembrow et al. 2010; Sheets et al. 2011; Avesar and Gulledge 2012). This suggests that L5 IT cells are more physiologically diverse than L5 PT cells in M2. Next, we compared the physiological properties of L5a cM2 cells including both ER81 positive and negative cells, and iPERp cells, most of which were positive for ER81, and their synaptic connections in M2 of adult mice. The cells were recorded deeper than 50 μm from the slice surface (Fig. 7A and B).

In adult mice, iPERp cells were lower in input resistance ($P < 0.001$, Mann-Whitney U test) and lower in its variance ($P < 0.001$, F test) than cM2p cells, which include iPERp cells (Fig. 7C, Table 1). The synaptic connectivity was investigated by simultaneous recording of two cells with a horizontal distance less than $\sim 60 \mu\text{m}$ ($35.0 \pm 11.9 \mu\text{m}$ for cM2p cell pairs; $33.2 \pm 7.7 \mu\text{m}$ for iPERp cell pairs, $P = 0.51$; Fig. 7D). The connection probability was higher in iPERp cell pairs (0.18; 12 out of 66 tested directions) than in cM2p cell pairs (0.085; 11 out of 129 tested directions; $P = 0.048$, chi-square test; Fig. 7E). The EPSC amplitude and paired-pulse ratio (interval: 100 ms) were similar between iPERp and cM2p cell pairs (Table 1). The difference in input resistance was larger for unconnected cM2p pairs than for unconnected iPERp pairs ($P < 0.001$), but not different between connected cM2p and iPERp pairs ($P = 0.83$; Fig. 7F). This indicates that L5 IT cells with similar input resistance are more connected locally. These suggest that iPER cells are connected to each other more often than common IT cells in L5a.

Discussion

We found that innervation preference for L1 of M2-L5 IT cells depends on their projection patterns to other areas as well as their gene expression and electrophysiological

properties, based on MouseLight database analysis, tracer labeling, ER81 immunohistochemistry, and in vitro electrophysiology. M2-L5a IT cells with stronger innervation preference for L1 extended their axons over more regions, including auditory and perirhinal cortices. The L1-preferring IT cells also projected to a larger volume of the striatum than did L1-nonpreferring cells. ER81 was expressed more in L1-preferring IT cells than other IT cells, and more in IT cells projecting to perirhinal/auditory cortex than those projecting to the primary motor or somatosensory cortices. The perirhinal cortex-projecting cells were lower in input resistance and higher in connection probability than the contralateral M2-projecting cells including both ER81-positive and -negative cells.

L5 IT cells in the frontal cortex are diverse not only in their molecular markers but also in the cortical areas they innervate. We found that these features were related in the murine, characterizing two distinct feedback projection channels from L5 IT cells in M2. We found that IT cells projecting to many cortical areas (broad projection IT cells) densely innervate L1 and express ER81 more frequently than do IT cells projecting to fewer cortical areas (restricted projection IT cells; Fig. 8). In L5a of M2, in addition to IT cells, there are PT cells projecting to M1, which innervate L1 like broad projection IT cells but do not innervate the perirhinal cortex like restricted projection IT cells (Fig. 8; Ueta et al. 2013; Ueta et al. 2014; Kawaguchi 2017). PT cells innervate less heterogeneous regions in the ipsilateral striatum than IT cells that project to the striatum bilaterally (Morita et al. 2019). Therefore, to fully understand the role of L5 corticocortical feedback from the frontal cortex to the lower-order areas, three distinct output channels (from broad projection IT, restricted projection IT, and PT cells) need to be analyzed independently. The proportion of IT cells among L5 PCs in association cortex is much higher in humans relative to mice (Hodge et al. 2019). Since the human prefrontal cortex projects to various areas of the temporoparietal cortex, proposed to be used to construct and manipulate mental models (Ito 2008), its broad projection IT cells are thought to be further differentiated with regard to their molecular expression and innervation patterns.

From the relationship between soma sublayer-distribution, innervation pattern, and ER81 expression in IT cells, we reasoned that L5a includes both ER81-positive broad projection and ER81-negative restricted projection IT cells, but L5b is mainly composed of the latter. In murine motor-related areas, IT cells projecting to distal cortical areas, such as auditory, perirhinal, and/or posterior parietal areas, are preferentially distributed in L5a, whereas projections from L5b cells were typically restricted to nearby areas (Fig. 5C; Ueta et al. 2013). This finding would be further confirmed if the axon distribution of L5a and L5b IT cells could be compared in the MouseLight database.

We found ER81 was more highly expressed in broad projection IT cells than in restricted projection IT cells.

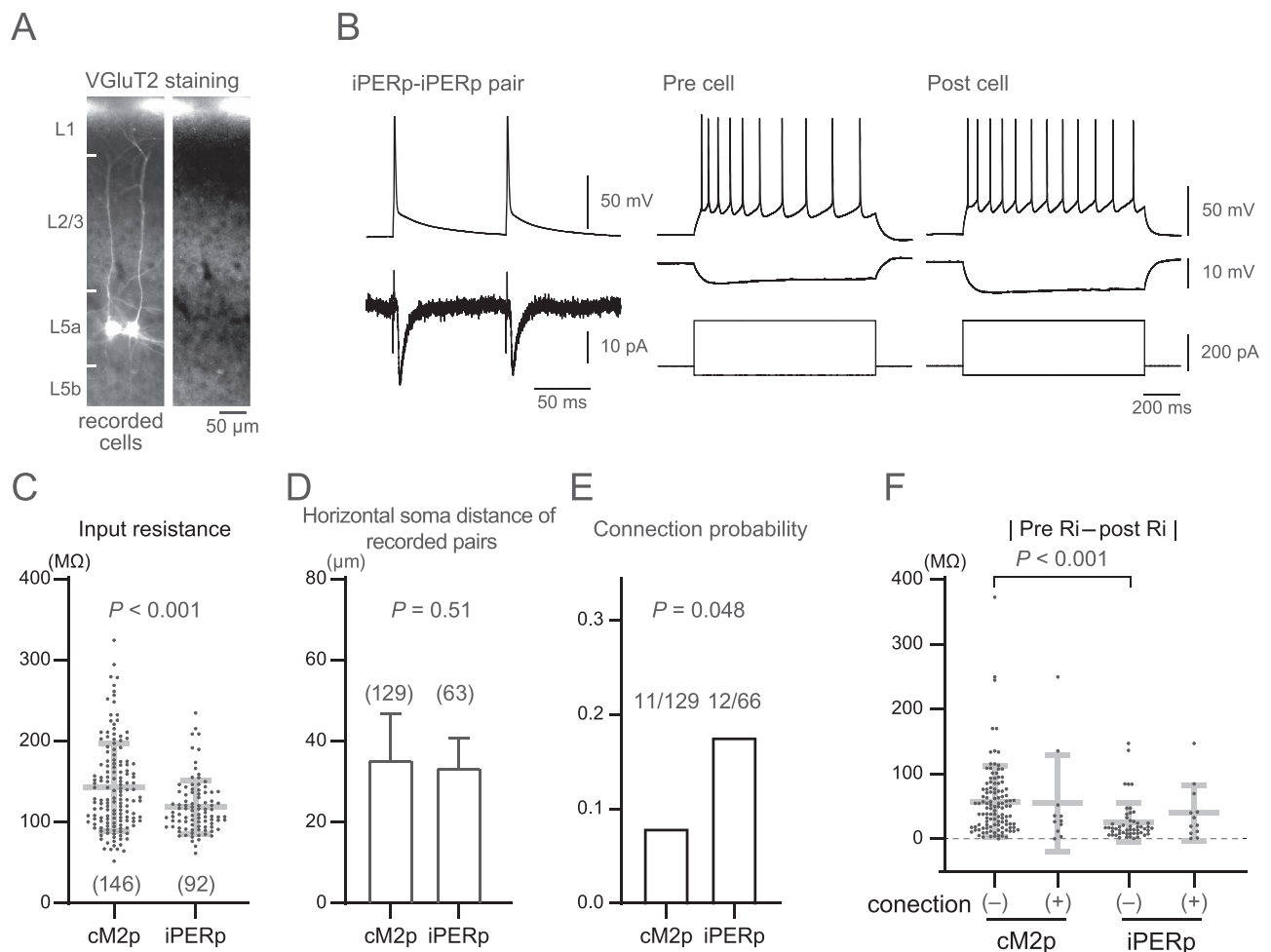


Fig. 7. Electrophysiological and connection properties of cM2p and iPERp cells in mouse M2. A) Simultaneously recorded cM2p cells in L5a. L5a was identified by weaker immunofluorescence for VGLuT2. B) EPSC induction in iPERp cell pairs. Left, two presynaptic spikes (interval, 100 ms) above and EPSCs in a postsynaptic cell below. Right, pre- and postsynaptic cell responses to depolarizing (250 pA, 1 s) and hyperpolarizing (−50 pA) current pulses. C) Input resistance (R_i) of cM2p and iPERp cells. (n), number of cells. P , Mann–Whitney U test. D) Horizontal distance of somata in recorded cell pairs. (n), number of synaptic directions tested. E) Connection probability in cM2p and iPERp cell pairs (129 and 66 directions, respectively). P , chi-square test. F) Input resistance (R_i) difference between simultaneously recorded cells without or with synaptic connections. R_i difference was smaller in unconnected iPERp pairs ($25.4 \pm 30.6 \text{ M}\Omega$, $n=52$) than unconnected cM2p pairs ($57.7 \pm 54.4 \text{ M}\Omega$, $n=114$; $P < 0.001$), but not different between connected cM2p and iPERp pairs ($54.6 \pm 74.4 \text{ M}\Omega$ for connected cM2p pairs, $n=11$; $39.9 \pm 42.7 \text{ M}\Omega$ for connected iPERp pairs, $n=12$; $P=0.83$).

Table 1. Electrophysiological properties of L5a IT cells of mouse M2.

	cM2p cell	iPERp cell	stat.
	(146 cells)	(92 cells)	
Adaptation index	0.52 ± 0.12	0.53 ± 0.10	$P=0.93$
RMP (mV)	-67.5 ± 3.2	-67.6 ± 2.6	$P=0.78$
Input resistance ($\text{M}\Omega$)	142.7 ± 54.2	118.9 ± 33.0	$P < 0.001$
Time constant (ms)	25.9 ± 8.8	23.6 ± 5.9	$P=0.075$
Voltage sag (mV)	3.6 ± 1.6	3.5 ± 1.4	$P=0.63$
	(11 pairs)	(12 pairs)	
EPSC amplitude (pA)	10.0 ± 4.3	10.3 ± 6.4	$P=0.83$
EPSC paired-pulse ratio	0.96 ± 0.20	1.00 ± 0.23	$P=0.83$

Whole cell recording with potassium gluconate-based internal solution. cM2p, contralateral secondary motor cortex-projecting; iPERp, ipsilateral perirhinal cortex-projecting. Adaptation index = $[-f-1 \text{ slope of last interspike interval}] / [-f-1 \text{ slope of third interspike interval}]$; larger index means “more slowly adapting”. RMP, resting membrane potential. Voltage sag, peak amplitude of hyperpolarizing event measured from the steady-state voltage evoked by -0.2 nA of current injection. EPSCs, paired recording between the same group of cells. EPSC paired-pulse ratio, 100 ms interval. Data are mean \pm SD. stat., Mann–Whitney U test.

In L5 of mouse M1, IT cells expressing *Fezf2* (Fez family zinc finger 2: another transcription factor) differ in their intrinsic physiological characteristics and dendritic morphology from those that are negative for *Fezf2*

(Tantirigama et al. 2014). *Fezf2*-positive IT cells are distributed in L5a, but *Fezf2*-negative cells are preferentially distributed in L5b. We found that the distribution of ER81-expression was similar: ER81-positive neurons were

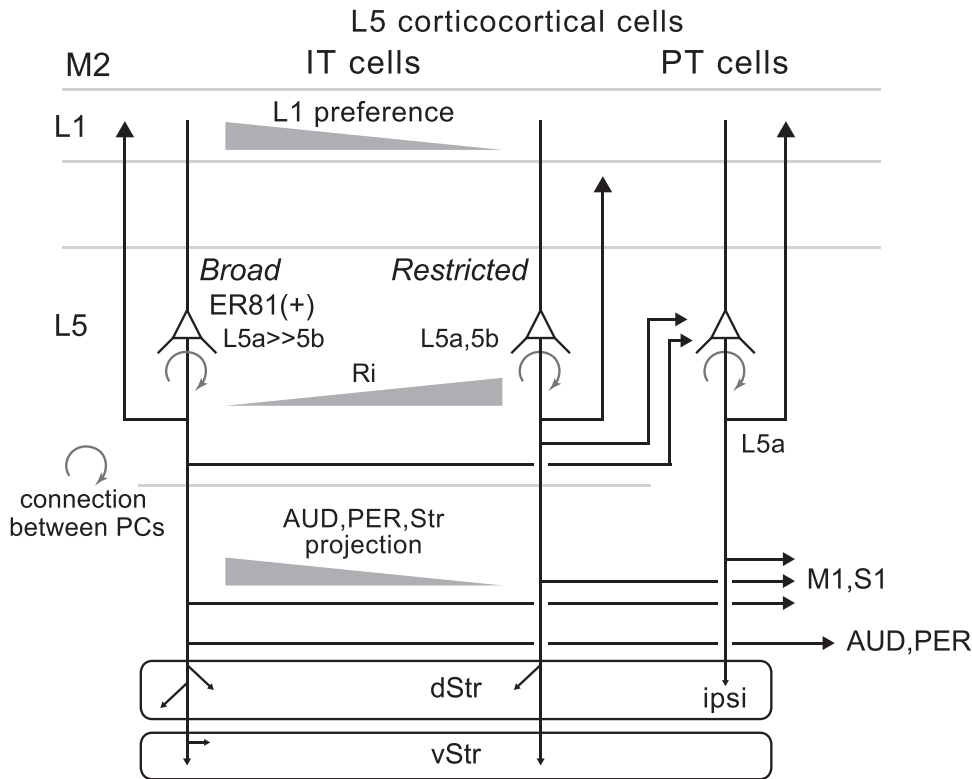


Fig. 8. Corticocortical innervation subtypes of M2-L5 pyramidal cells. Broad projection IT cells target more diverse cortical and striatal areas, innervate L1 more densely, and express ER81 more frequently than restricted projection IT cells. L5a PT cells innervate L1, like broad IT cells. They project to M1 but not to the perirhinal cortex, like restricted IT cells. IT cells innervate bilateral dorsal and ventral striatum, but PT cells only ipsilateral striatum.

preferentially found in L5a (Fig. 5B). Since L5 IT cells expressing *Fezf2* in anterior lateral motor cortex do not necessarily express ER81 (Tasic et al. 2018), *Fezf2*-positive cells may partially overlap with ER81-positive broad projection IT cells.

ER81-positive cM2p cells were much more abundant in L5a than L5b in mouse M2. This sublayer-preferential distribution of ER81 cells is consistent with previous studies in mice (Watakabe et al. 2007; Groh et al. 2010). The proportion of ER81 cells in L5a cM2p cells was about the same in mice and rats, but L5b cM2p cells positive for ER81 were more common in rats than mice. Thus, L5b IT cells show different ER81 expression patterns in mice and rats. Furthermore, the laminar distribution of ER81 depends upon cortical region in mouse (Hirokawa et al. 2008). ER81 is expressed in both IT and PT cells. Therefore, ER81 expression in L1-preferring/broad projection IT cells of L5a is not directly related to the determination of innervation patterns.

In M2-L5, pairs of synaptically connected IT cells exhibit similar dendritic morphologies and electrophysiological properties, leading to the formation of subnetworks having similar intrinsic properties (Morishima and Kawaguchi 2006; Otsuka and Kawaguchi 2011). Our results further suggest that these subnetworks may also share cortical area- and layer-innervation patterns.

M2 PT cells innervate L1 of frontal cortex (Ueta et al. 2013; Ueta et al. 2014), and L1 is also innervated by

thalamic nuclei receiving output from the basal ganglia (Kuramoto et al. 2009; Rubio-Garrido et al. 2009; Shigematsu et al. 2016; Tanaka et al. 2018). On the other hand, broad projection IT cells innervate L1 in frontal areas and also in multiple sensory areas that are not directly related to basal ganglia output. PT cells preferentially innervate the upper part of L1 (L1a), while IT cells innervate L1 more uniformly (Hirai et al. 2012; Ueta et al. 2013). Thus, these L5 cell subtypes may affect L1 circuit function differently.

We found that some M2-L5 IT cells preferentially innervate L1 in both the proximal and distal cortical regions, but that others preferentially target other layers containing PC somata and basal/oblique dendrites in proximal regions. Thick-tufted PCs of L5 generate bursts of action potentials in response to simultaneous excitation of their apical tuft and soma (Larkum et al. 1999; Williams and Stuart 1999; Larkum and Zhu 2002). Thus, M2-L5 afferents from both broad and restricted projection IT cells as well as from L5a PT cells might induce burst firing in L5 PCs in proximal cortical regions, such as M1 and S1, by providing input to both L1 and L5. In distal cortical regions, like AUD and PER, burst firing in response to broad projection IT afferents from M2-L5 to L1 would require additional input from other excitatory inputs to the basal/oblique dendrites of PCs. Thus, L5 PCs of the frontal cortex have multiple feedback channels that can have different excitatory effects on the PCs, depending on the target.

Acknowledgments

The mouse line Tlx3-Cre PL56 was kindly provided by Charles Gerfen and Nathaniel Heintz, VGAT-tdTomato by Yuchio Yanagawa, and a rabbit antibody against mouse ER81 by Thomas Jessell. We thank Yasuhiro Tanaka, Yoshiyuki Kubota, and Allan T. Gulledge for helpful discussions, and Fransiscus A. Agahari and Steven R. Vincent for comments. This was supported by the Cooperative Study Program of National Institute for Physiological Sciences (Section of Electron Microscopy).

Supplementary material

Supplementary material is available at *Cerebral Cortex* Journal online.

Funding

This work was supported by Grant-in-Aids for Scientific Research from the Ministry of Education, Culture, Sports, Science, and Technology/Japan Society for the Promotion of Science (KAKENHI No., 17H06311 and 20H03359 to YK; 20H05049 to KM).

Conflict of interest statement. None declared.

Author Contributions

SI and YK conceived and designed the experiments, analyzed the data, and wrote the article. SI, MY, KM and YK analyzed the MouseLight database. YU, TO, MM, YH and YK reanalyzed the previous electrophysiological data of rats. KK and RK provided the research material. All of the authors revised and approved the manuscript.

References

- Arber S, Ladle DR, Lin JH, Frank E, Jessell TM. ETS gene *Er81* controls the formation of functional connections between group Ia sensory afferents and motor neurons. *Cell*. 2000;101:485–498.
- Arlotta P, Molyneaux BJ, Chen J, Inoue J, Kominami R, Macklis JD. Neuronal subtype-specific genes that control corticospinal motor neuron development in vivo. *Neuron*. 2005;45:207–221.
- Avesar D, Gulledge AT. Selective serotonergic excitation of callosal projection neurons. *Front Neural Circuits*. 2012;6:12.
- Baker A, Kalmbach B, Morishima M, Kim J, Juavinett A, Li N, Dembrow N. Specialized subpopulations of deep-layer pyramidal neurons in the neocortex: bridging cellular properties to functional consequences. *J Neurosci*. 2018;38:5441–5455.
- Barbas H. General cortical and special prefrontal connections: principles from structure to function. *Annu Rev Neurosci*. 2015;38:269–289.
- Barbas H, Rempel-Clower N. Cortical structure predicts the pattern of corticocortical connections. *Cereb Cortex*. 1997;7:635–646.
- Barthas F, Kwan AC. Secondary motor cortex: where 'sensory' meets 'motor' in the rodent frontal cortex. *Trends Neurosci*. 2017;40:181–193.
- Bastos AM, Usrey WM, Adams RA, Mangun GR, Fries P, Friston KJ. Canonical microcircuits for predictive coding. *Neuron*. 2012;76:695–711.
- Dembrow NC, Chitwood RA, Johnston D. Projection-specific neuromodulation of medial prefrontal cortex neurons. *J Neurosci*. 2010;30:16922–16937.
- D'Souza RD, Burkhalter A. A laminar organization for selective cortico-cortical communication. *Front Neuroanat*. 2017;11:71.
- Economo MN, Clack NG, Lavis LD, Gerfen CR, Svoboda K, Myers EW, Chandrashekar J. A platform for brain-wide imaging and reconstruction of individual neurons. *elife*. 2016;5:e10566.
- Felleman DJ, Van Essen DC. Distributed hierarchical processing in the primate cerebral cortex. *Cereb Cortex*. 1991;1:1–47.
- Gerfen CR, Paletzki R, Heintz N. GENSAT BAC cre-recombinase driver lines to study the functional organization of cerebral cortical and basal ganglia circuits. *Neuron*. 2013;80:1368–1383.
- Groh A, Meyer HS, Schmidt EF, Heintz N, Sakmann B, Krieger P. Cell-type specific properties of pyramidal neurons in neocortex underlying a layout that is modifiable depending on the cortical area. *Cereb Cortex*. 2010;20:826–836.
- Harb K, Magrinelli E, Nicolas CS, Lukianets N, Frangeul L, Pietri M, Sun T, Sandoz G, Grammont F, Jabaudon D, et al. Area-specific development of distinct projection neuron subclasses is regulated by postnatal epigenetic modifications. *Elife*. 2016;5:e09531.
- Harris KD, Shepherd GM. The neocortical circuit: themes and variations. *Nat Neurosci*. 2015;18:170–181.
- Harris JA, Mihalas S, Hirokawa KE, Whitesell JD, Choi H, Bernard A, Bohn P, Caldejon S, Casal L, Cho A, et al. Hierarchical organization of cortical and thalamic connectivity. *Nature*. 2019;575:195–202.
- Harwell CC, Parker PR, Gee SM, Okada A, McConnell SK, Kreitzer AC, Kriegstein AR. Sonic hedgehog expression in corticofugal projection neurons directs cortical microcircuit formation. *Neuron*. 2012;73:1116–1126.
- Hattox AM, Nelson SB. Layer V neurons in mouse cortex projecting to different targets have distinct physiological properties. *J Neurophysiol*. 2007;98:3330–3340.
- Hirai Y, Morishima M, Karube F, Kawaguchi Y. Specialized cortical subnetworks differentially connect frontal cortex to parahippocampal areas. *J Neurosci*. 2012;32:1898–1913.
- Hirokawa J, Watakabe A, Ohsawa S, Yamamori T. Analysis of area-specific expression patterns of RORbeta, ER81 and Nurr1 mRNAs in rat neocortex by double in situ hybridization and cortical box method. *PLoS One*. 2008;3:e3266.
- Hodge RD, Bakken TE, Miller JA, Smith KA, Barkan ER, Graybuck LT, Close JL, Long B, Johansen N, Penn O, et al. Conserved cell types with divergent features in human versus mouse cortex. *Nature*. 2019;573:61–68.
- Hooks BM, Papale AE, Paletzki RF, Feroze MW, Eastwood BS, Couey JJ, Winnubst J, Chandrashekar J, Gerfen CR. Topographic precision in sensory and motor corticostriatal projections varies across cell type and cortical area. *Nat Commun*. 2018;9:3549.
- Ito M. Control of mental activities by internal models in the cerebellum. *Nat Rev Neurosci*. 2008;9:304–313.
- Kaneko R, Takatsuru Y, Morita A, Amano I, Haijima A, Imayoshi I, Tamamaki N, Koibuchi N, Watanabe M, Yanagawa Y. Inhibitory neuron-specific Cre-dependent red fluorescent labeling using VGAT BAC-based transgenic mouse lines with identified transgene integration sites. *J Comp Neurol*. 2018;526:373–396.
- Kawaguchi Y. Groupings of nonpyramidal and pyramidal cells with specific physiological and morphological characteristics in rat frontal cortex. *J Neurophysiol*. 1993;69:416–431.

- Kawaguchi Y. Pyramidal cell subtypes and their synaptic connections in layer 5 of rat frontal cortex. *Cereb Cortex*. 2017;27:5755–5771.
- Kincaid AE, Zheng T, Wilson CJ. Connectivity and convergence of single corticostriatal axons. *J Neurosci*. 1998;18:4722–4731.
- Kiritani T, Wickersham IR, Seung HS, Shepherd GM. Hierarchical connectivity and connection-specific dynamics in the corticospinal-corticostriatal microcircuit in mouse motor cortex. *J Neurosci*. 2012;32:4992–5001.
- Kuan L, Li Y, Lau C, Feng D, Bernard A, Sunkin SM, Zeng H, Dang C, Hawrylycz M, Ng L. Neuroinformatics of the allen mouse brain connectivity atlas. *Methods*. 2015;73:4–17.
- Kuramoto E, Furuta T, Nakamura KC, Unzai T, Hioki H, Kaneko T. Two types of thalamocortical projections from the motor thalamic nuclei of the rat: a single neuron-tracing study using viral vectors. *Cereb Cortex*. 2009;19:2065–2077.
- Larkum ME, Zhu JJ. Signaling of layer 1 and whisker-evoked Ca^{2+} and Na^{+} action potentials in distal and terminal dendrites of rat neocortical pyramidal neurons in vitro and in vivo. *J Neurosci*. 2002;22:6991–7005.
- Larkum ME, Zhu JJ, Sakmann B. A new cellular mechanism for coupling inputs arriving at different cortical layers. *Nature*. 1999;398:338–341.
- Lin HM, Kuang JX, Sun P, Li N, Lv X, Zhang YH. Reconstruction of intratelencephalic neurons in the mouse secondary motor cortex reveals the diverse projection patterns of single neurons. *Front Neuroanat*. 2018;12:86.
- Madisen L, Zwingman TA, Sunkin SM, Oh SW, Zariwala HA, Gu H, Ng LL, Palmiter RD, Hawrylycz MJ, Jones AR, et al. A robust and high-throughput Cre reporting and characterization system for the whole mouse brain. *Nat Neurosci*. 2010;13:133–140.
- Makino H, Ren C, Liu H, Kim AN, Kondapaneni N, Liu X, Kuzum D, Komiyama T. Transformation of cortex-wide emergent properties during motor learning. *Neuron*. 2017;94:880–890 e888.
- Manita S, Suzuki T, Homma C, Matsumoto T, Odagawa M, Yamada K, Ota K, Matsubara C, Inutsuka A, Sato M, et al. A top-down cortical circuit for accurate sensory perception. *Neuron*. 2015;86:1304–1316.
- Markov NT, Vezoli J, Chameau P, Falchier A, Quilodran R, Huissoud C, Lamy C, Misery P, Giroud P, Ullman S, et al. Anatomy of hierarchy: feedforward and feedback pathways in macaque visual cortex. *J Comp Neurol*. 2014;522:225–259.
- Mejias JF, Murray JD, Kennedy H, Wang XJ. Feedforward and feedback frequency-dependent interactions in a large-scale laminar network of the primate cortex. *Sci Adv*. 2016;2:e1601335.
- Molyneaux BJ, Arlotta P, Fame RM, MacDonald JL, MacQuarrie KL, Macklis JD. Novel subtype-specific genes identify distinct subpopulations of callosal projection neurons. *J Neurosci*. 2009;29:12343–12354.
- Morishima M, Kawaguchi Y. Recurrent connection patterns of corticostriatal pyramidal cells in frontal cortex. *J Neurosci*. 2006;26:4394–4405.
- Morishima M, Morita K, Kubota Y, Kawaguchi Y. Highly differentiated projection-specific cortical subnetworks. *J Neurosci*. 2011;31:10380–10391.
- Morita K, Im S, Kawaguchi Y. Differential striatal axonal arborizations of the intratelencephalic and pyramidal-tract neurons: analysis of the data in the MouseLight database. *Front Neural Circuits*. 2019;13:71.
- Otsuka T, Kawaguchi Y. Firing-pattern-dependent specificity of cortical excitatory feed-forward subnetworks. *J Neurosci*. 2008;28:11186–11195.
- Otsuka T, Kawaguchi Y. Cell diversity and connection specificity between callosal projection neurons in the frontal cortex. *J Neurosci*. 2011;31:3862–3870.
- Ramaswamy S, Markram H. Anatomy and physiology of the thick-tufted layer 5 pyramidal neuron. *Front Cell Neurosci*. 2015;9:233.
- Rubio-Garrido P, Perez-de-Manzo F, Porrero C, Galazo MJ, Clasca F. Thalamic input to distal apical dendrites in neocortical layer 1 is massive and highly convergent. *Cereb Cortex*. 2009;19:2380–2395.
- Sheets PL, Suter BA, Kiritani T, Chan CS, Surmeier DJ, Shepherd GM. Corticospinal-specific HCN expression in mouse motor cortex: I(h)-dependent synaptic integration as a candidate microcircuit mechanism involved in motor control. *J Neurophysiol*. 2011;106:2216–2231.
- Shigematsu N, Ueta Y, Mohamed AA, Hatada S, Fukuda T, Kubota Y, Kawaguchi Y. Selective thalamic innervation of rat frontal cortical neurons. *Cereb Cortex*. 2016;26:2689–2704.
- Shipp S. The importance of being agranular: a comparative account of visual and motor cortex. *Philos Trans R Soc Lond Ser B Biol Sci*. 2005;360:797–814.
- Shipp S, Adams RA, Friston KJ. Reflections on agranular architecture: predictive coding in the motor cortex. *Trends Neurosci*. 2013;36:706–716.
- Tanaka YH, Tanaka YR, Kondo M, Terada SI, Kawaguchi Y, Matsuzaki M. Thalamocortical axonal activity in motor cortex exhibits layer-specific dynamics during motor learning. *Neuron*. 2018;100:244, e212–258.
- Tantirigama ML, Oswald MJ, Duynstee C, Hughes SM, Empson RM. Expression of the developmental transcription factor Fezf2 identifies a distinct subpopulation of layer 5 intratelencephalic-projection neurons in mature mouse motor cortex. *J Neurosci*. 2014;34:4303–4308.
- Tasic B, Yao Z, Graybiel LT, Smith KA, Nguyen TN, Bertagnoli D, Goldy J, Garren E, Economo MN, Viswanathan S, et al. Shared and distinct transcriptomic cell types across neocortical areas. *Nature*. 2018;563:72–78.
- Ueta Y, Hirai Y, Otsuka T, Kawaguchi Y. Direction- and distance-dependent interareal connectivity of pyramidal cell subpopulations in the rat frontal cortex. *Front Neural Circuits*. 2013;7:164.
- Ueta Y, Otsuka T, Morishima M, Ushimaru M, Kawaguchi Y. Multiple layer 5 pyramidal cell subtypes relay cortical feedback from secondary to primary motor areas in rats. *Cereb Cortex*. 2014;24:2362–2376.
- Ueta Y, Sohn J, Agahari FA, Im S, Hirai Y, Miyata M, Kawaguchi Y. Ipsi- and contralateral corticocortical projection-dependent subcircuits in layer 2 of the rat frontal cortex. *J Neurophysiol*. 2019;122:1461–1472.
- Ushimaru M, Kawaguchi Y. Temporal structure of neuronal activity among cortical neuron subtypes during slow oscillations in anesthetized rats. *J Neurosci*. 2015;35:11988–12001.
- Wang Q, Ding SL, Li Y, Royall J, Feng D, Lesnar P, Graddis N, Naeemi M, Facer B, Ho A, et al. The allen mouse brain common coordinate framework: a 3D reference atlas. *Cell*. 2020;181:936, e920–953.
- Watakabe A, Ichinohe N, Ohsawa S, Hashikawa T, Komatsu Y, Rockland KS, Yamamori T. Comparative analysis of layer-specific genes in mammalian neocortex. *Cereb Cortex*. 2007;17:1918–1933.
- Williams SR, Stuart GJ. Mechanisms and consequences of action potential burst firing in rat neocortical pyramidal neurons. *J Physiol*. 1999;521(Pt 2):467–482.
- Wilson CJ, Groves PM, Kitai ST, Linder JC. Three-dimensional structure of dendritic spines in the rat neostriatum. *J Neurosci*. 1983;3:383–388.

- Winnubst J, Bas E, Ferreira TA, Wu Z, Economo MN, Edson P, Arthur BJ, Bruns C, Rokicki K, Schauder D, et al. Reconstruction of 1,000 projection neurons reveals new cell types and organization of long-range connectivity in the mouse brain. *Cell*. 2019;179:268, e213–281.
- Yeterian EH, Pandya DN, Tomaiuolo F, Petrides M. The cortical connectivity of the prefrontal cortex in the monkey brain. *Cortex*. 2012;48:58–81.
- Yoneshima H, Yamasaki S, Voelker CC, Molnar Z, Christophe E, Audinat E, Takemoto M, Nishiwaki M, Tsuji S, Fujita I, et al. Er81 is expressed in a subpopulation of layer 5 neurons in rodent and primate neocortices. *Neuroscience*. 2006;137:401–412.
- Zheng T, Wilson CJ. Corticostriatal combinatorics: the implications of corticostriatal axonal arborizations. *J Neurophysiol*. 2002;87:1007–1017.